AN $H(\mathbf{div}, \Omega)$-CONFORMING FLUX RECONSTRUCTION FOR THE MULTISCALE HYBRID-MIXED METHOD

GABRIEL R. BARRENECHEA, LARISSA MARTINS, FRÉDÉRIC VALENTIN, AND FRÉDÉRIC VALENTIN

Abstract. The Multiscale Hybrid-Mixed (MHM) method is a multiscale finite element method based on a hybrid weak formulation, originally proposed for problems linked to flow in porous media. Its starting point is a variational formulation that guarantees that the flux variable is $H(\mathrm{div};\Omega)$-conforming. This property is lost when the local problems, in their elliptic form, are discretized using primal finite element methods. In this work, we close that gap by proposing and analyzing a new flux reconstruction for the MHM method, computed element-wise on submeshes, that belongs to $H(\mathrm{div};\Omega)$. The reconstruction converges optimally in the $L^2(\Omega)-$norm. Furthermore, the divergence of the reconstructed flow is the piecewise continuous polynomial projection of the source term onto submeshes and thus it also converges optimally in the $L^2(\Omega)-$norm. As a by-product of the reconstruction technique, a fully computable *a posteriori* error estimator is presented and analyzed. These theoretical results are validated experimentally via numerical computations.

1. Introduction

Multiscale finite element methods have seen significant advancements in recent decades, both theoretically and practically. They are known to be accurate without resolving fine scales through multiscale functions computed from decoupled problems which take advantage of massively parallel computers efficiently. Since the seminal work [7], there has been vast literature on the subject. In the context of the Darcy model (or Poisson equation), several alternatives have been proposed over the last two decades, such as the VMS method [33], MsFEM and GMsFEM [21], the PGEM and GEM [8, 28], the HMM [1], Multiscale Mortar method [6], the LOD method [38] and the LSD method [37], just to cite a few (see, e.g., [36] for a recent review). This work focuses on the Multiscale Hybrid-Mixed (MHM for short) method [31, 4]. The MHM method is a by-product of a hybrid formulation that starts at the continuous level posed on a coarse partition of the domain. It consists of decomposing the exact solution into local and global contributions. When discretized, such a characterization decouples local and global problems: the global formulation involves only degrees of freedom over the skeleton of the coarse partition, while the local problems provide the multiscale basis functions. Interestingly, the multiscale basis functions can be computed locally through independent problems. Local problems can be solved using primal finite element methods, as in [30, 9], or using mixed methods such as in [20].

The choice of method is guided by the physical quantities of interest. Fluxes and stresses often constitute the primary variables of interest in various applications, including heat conduction, percolation in porous media, and stress analysis [35]. The classical way of obtaining an accurate flux for the Darcy problem is by introducing a mixed (or hybrid) formulation and solve it using appropriate mixed finite element methods. The use of local mixed problems in the MHM method (see [20]) gives an accurate $H(\mathrm{div};\Omega)-$conforming flux variable, but incurs increased computational cost. On the other hand, using a primal finite element method as a second-level solver in the MHM method [30, 9]

is computationally attractive, but fails to preserve the $H(\mathrm{div};\Omega)-$conformity. One alternative is to perform an accurate $H(\mathrm{div};\Omega)-$conforming flow reconstruction using the discrete solution for primal finite element methods locally. The ability to perform such reconstruction element-wisely using the primal discrete solution is particularly attractive from a computational standpoint and has been proposed for standard finite element and discontinuous Galerkin methods in [44] and [26, 25], respectively. The flux can also be post-processed from the vertex-patch-wise approach, as detailed in works such as [11, 18, 24]. Additionally, fluxes can also be utilized in *a posteriori* error estimates reliant on equilibrated fluxes for primal formulations [24]. Consequently, in applications such as porous media flow, where $\boldsymbol{\sigma} := -A\nabla u$ denotes the Darcy velocity, it is important that the flux $\boldsymbol{\sigma}$, in addition to being accurate, belongs to $H(\mathrm{div};\Omega)$ (see, e.g., [17] for an example). This last requirement is of importance, on the one hand, because the continuity of the normal components of the flux guarantees conservation, and on the other, because the normal component of the flux is the natural input to model the transport phenomena.

In this work we take the path where an $H(\mathrm{div};\Omega)-$conforming flux is built starting from the solution of the MHM formulation as a post-processing step, provided that the multiscale basis function are not computed exactly. We build up on the ideas presented in [15, 17, 44], though none of them have a submesh on the macro elements. We use local Raviart-Thomas spaces (c.f. [42]) so that the reconstructed flux has continuous normal components in submeshes and is conservative in each macro element, even though the reconstruction is carried out locally in the submesh. The presence of the submeshes associated with the skeleton of the global partition and local problems in the MHM method makes the extension of previous strategies nontrivial, as special care needs to be taken to guarantee the normal continuity in the interior facets of the subtriangulation (that is, the ones that are not associated to global degrees of freedom) while maintaining the accuracy of the original discrete solution. Due to the local character of the reconstruction, the computational overhead is negligible, while it produces an optimally convergent flux in the $L^2(\Omega)$-norm and $H(\mathrm{div};\Omega)$-norm. In addition, thanks to the nature of the MHM method, we prove that the divergence of the reconstructed flux in the macro element is the projection of the right-hand side datum onto the continuous finite element space used in the second-level computation. Hence, the projection of the divergence of the reconstructed flux exhibits optimal convergence with respect to the local mesh parameter. Moreover, if the submesh coincides with the coarse-scale one (i.e., a submesh consisting of only one element), then the divergence itself converges optimally. The vertex-patch-wise approach [40] is an alternative to achieve local mass conservation in the submesh elements (see also [20]) at the price of solving mixed problems on patches of elements. Such an approach leads to $p-$robust error estimates (see also [14] for more general cases), a study that is out of the scope of the present work.

As mentioned above, flux reconstructions have been linked to the development of *a posteriori* error estimators. Up to our best knowledge, the first *a posteriori* error estimator that used this idea was proposed in [41], and similar ideas have been applied since then in different contexts (see [27, 12]). Particularly attractive is the *a posteriori* error estimation in [40] that relies on post-processed flux and potential reconstruction from the vertex-patch-wise approach, extending ideas from the Prager-Synge equality [41]. The estimators provide guaranteed upper bounds on the energy error and are locally efficient, while also providing lower bounds, under the assumption that the numerical discretization satisfies a set of assumptions strongly tied to mixed finite element methods. Unfortunately, this scope (e.g. [40, Section 3.3]) cannot be directly used for the analysis of fully computable error estimators for

the MHM method based on second-level primal solvers, unlike MHM methods that rely on mixed local problems [10].

In the second part of this work, we derive a fully computable *a posteriori* error estimator for the MHM method. For that, we use the recovered flux variable of the first part of this work and the potential reconstruction using the Oswald averaging interpolation technique combined with the technique presented in [24]. The Oswald operator enforces continuity by averaging values across element interfaces, making it computationally efficient as it avoids the calculation of local, or global, projections to estimate the lack of $H^1(\Omega)$-conformity. As a result, we obtain a computable quantity that is a strict upper bound for the discretization error of the MHM method. The estimators constructed in this manner are defined as the norm of the difference between the gradient of the primal variable, multiplied by the physical coefficient, and the reconstructed flux, as well as the norm of the difference between the gradient of the primal variable and that derived from the reconstructed potential. In addition, the estimators include a new term that measures the local lack of conservation of the MHM solution on submesh elements due to the choice of local primal finite element solvers to approximate the multiscale basis.

The proposed *a posteriori* estimator also provides a lower bound for the discretization error of the MHM method. The expression used as discretization error for the lower bound has more terms than the one used for the upper bound, which classifies the estimator as weakly efficient. Interestingly, [40] provides a local efficient estimator for multiscale methods using patch-wise flux reconstructions, where local Neumann problems are solved using rotated gradients. Unfortunately, the lower bound for our proposed multiscale error estimator and the one proposed in [40] share the shortcoming of depending on the ratio between local and global mesh parameters. As such, constructing robust estimators for multiscale methods (from the point of view of local efficiency) remains an open problem (see also [13]).

The rest of the paper is organized as follows. In Section 2, the main notations, model problem, and preliminary results are presented. The MHM method is presented in Section 3, and the flux recovery is presented and analyzed in Section 4. In Section 5, we derive the *a posteriori* error estimator, and numerical experiments validating the theoretical results are given in Section 6. Some conclusions are drawn in Section 7, and in Appendix A we prove some technical results needed for the error analysis.

2. Setting and Preliminary Results

This section introduces the model problem and its hybrid formulation, and a characterization of the exact solution with respect to the solution of global-local boundary value problems. It follows closely previous works on the MHM method [4, 9].

2.1. **Model Problem.** Let $\Omega \subset \mathbb{R}^d$, $d \in \{2, 3\}$, be an open, bounded, and connected polytope with Lipschitz boundary $\partial\Omega$. Given $f \in L^2(\Omega)$ and $g \in H^{1/2}(\partial\Omega)$, we define the following boundary value problem: Find $u \in H^1(\Omega)$ such that $u|_{\partial\Omega} = g$ and

$$\int_\Omega A\nabla u \cdot \nabla v = \int_\Omega f\, v \quad \text{for all } v \in H^1_0(\Omega)\,. \tag{2.1}$$

Here, $A \in L^\infty(\Omega)^{d\times d}$ is a symmetric matrix and may involve *multiscale* features that will be assumed to be regular enough so its traces on the facets of the triangulation are well-defined. We will impose more precise regularity assumptions on it later. It is also supposed to be uniformly elliptic in Ω. More

precisely, we assume that there exist positive constants $A_{\min}$ and $A_{\max}$ such that

$$A_{\min}|\boldsymbol{\xi}|^2 \leq \boldsymbol{\xi}^T A(\boldsymbol{x})\boldsymbol{\xi} \leq A_{\max}|\boldsymbol{\xi}|^2 \quad \text{for all } \boldsymbol{\xi} \in \mathbb{R}^d\,, \tag{2.2}$$

and for almost all $\boldsymbol{x} \in \Omega$, where $|\cdot|$ is the Euclidian norm. The standard weak formulation (2.1) is a well-posed problem (c.f. [23, Example 25.4]).

Above and hereafter we will adopt standard notation for Sobolev and Lebesgue spaces aligned with, e.g., [22], where $H^s(D)$ ($L^2(D) = H^0(D)$) stands for the usual Sobolev spaces on an open bounded set $D \subset \mathbb{R}^d$, $d \in \{1, 2, 3\}$ and $s \in \mathbb{R}$. As usual, $H^1_0(D)$ is the space of functions in $H^1(D)$ with null trace in ∂D. We also denote by $(\cdot,\cdot)_D$ the $L^2(D)$-inner product (we do not make a distinction between vector-valued and scalar-valued functions), i.e.,

$$(f, g)_D = \int_D f\, g\,.$$

Finally, the product $\langle\cdot,\cdot\rangle_{\partial D}$ denotes the duality pairing between $H^{-1/2}(\partial D)$ and $H^{1/2}(\partial D)$. Also, $\|\cdot\|_{s,D}$ and $|\cdot|_{s,D}$ are the usual norm and semi-norm in $H^s(D)$, for every integer $s \geq 1$.

The dual variable associated to (2.1) is $\boldsymbol{\sigma} := -A\nabla u$, what we hereafter denote by flux. In a distributional sense, the flux satisfies the equation $\nabla\cdot\boldsymbol{\sigma} = f$ in Ω, which could be seen as an alternative formulation for the model problem. Due to the assumptions on u, A and f, the flux $\boldsymbol{\sigma}$ belongs to $H(\mathrm{div};\Omega)$, the space of functions in $L^2(\Omega)^d$ with divergence in $L^2(\Omega)$.

2.2. **Hybridization.** Following closely the presentation in [9], we start introducing $\mathscr{P}$, a collection of closed, bounded, disjoint polytopes, K, such that $\bar{\Omega} = \cup_{K\in\mathscr{P}} K$. The shapes of the polytopes K are, *a priori*, arbitrary, but we suppose that they satisfy a minimal angle condition (see Assumption A, Subsection 3.1, for a more precise statement). The diameter of K is $\mathcal{H}_K$ and we denote $\mathcal{H} = \max_{K\in\mathscr{P}} \mathcal{H}_K$. For each $K \in \mathscr{P}$, $\boldsymbol{n}^K$ denotes the unit outward normal to ∂K, such that $\boldsymbol{n}^K = \boldsymbol{n}$ on $\partial\Omega$ where, $\boldsymbol{n}$ is the unit outward normal to $\partial\Omega$. We also introduce $\partial\mathscr{P}$ as the set of boundaries ∂K, $\mathcal{E}$ the set of the faces in $\mathscr{P}$, and $\mathcal{E}_0$ the set of internal faces. By $\boldsymbol{n}_E$, we denote a unit normal vector on faces $E \in \mathcal{E}$, and $\boldsymbol{n}^K_E$ the unit outward normal vector on E with respect to K.

Now, given a partition $\mathscr{P}$ of Ω, for $m \geq 1$ we define the broken Sobolev space

$$H^m(\mathscr{P}) := \{v : v|_K \in H^m(K),\, \forall\, K \in \mathscr{P}\} \text{ with norm } \|v\|^2_{m,\mathscr{P}} := \sum_{K\in\mathscr{P}} \|v\|^2_{m,K}\,,$$

and we denote the respective semi-norm by $|\cdot|_{m,\mathscr{P}}$. In addition, the following spaces will be useful in what follows

$$\begin{aligned} V &:= H^1(\mathscr{P})\,,\\ V_0 &:= \{v \in V \,:\, v|_K \in \mathbb{P}_0(K) \text{ for all } K \in \mathscr{P}\}\,, \end{aligned}$$

where $\mathbb{P}_0(K)$ stands for the space of constants functions in K,

$$\tilde{V} := \{v \in V \,:\, v|_K \in H^1(K) \cap L^2_0(K),\, K \in \mathscr{P}\}\,,$$

where $L^2_0(K)$ represents the subspace of $L^2(K)$ consisting of functions with zero mean value in K. In addition, we define

$$\Lambda := \{\boldsymbol{\tau}\cdot\boldsymbol{n}^K|_{\partial K} \,:\, \boldsymbol{\tau} \in H(\mathrm{div};\Omega) \text{ for all } K \in \mathscr{P}\}\,.$$

Over the spaces V and Λ we define the respective norms

(2.3)
$$\|v\|_V := \left\{ \sum_{K\in\mathscr{P}} \frac{1}{d_\Omega^2}\|v\|_{0,K}^2 + \|\nabla v\|_{0,K}^2 \right\}^{1/2} \text{ and } \|\mu\|_\Lambda := \inf_{\substack{\boldsymbol{\tau}\in H(\mathrm{div};\Omega)\\ \boldsymbol{\tau}\cdot\boldsymbol{n}^K=\mu \text{ on } \partial K}} \|\boldsymbol{\tau}\|_{\mathrm{div},\Omega}\,,$$

where $d_\Omega > 0$ is the diameter of Ω and $H(\mathrm{div};\Omega) := \{\boldsymbol{\tau} \in L^2(\Omega)^d \,:\, \nabla\cdot\boldsymbol{\tau} \in L^2(\Omega)\}$ with norm

$$\|\boldsymbol{\tau}\|_{\mathrm{div},\Omega} := \left\{ \sum_{K\in\mathscr{P}} \|\boldsymbol{\tau}\|_{0,K}^2 + d_\Omega^2\|\nabla\cdot\boldsymbol{\tau}\|_{0,K}^2 \right\}^{1/2}. \tag{2.4}$$

Let $[\![v]\!]$ represent the jump of v on $E \in \mathcal{E}$, i.e., for two elements K and K' sharing E, we define

$$[\![v]\!]|_E := v|_K - v|_{K'} \quad \text{on } E \in \mathcal{E}_0\,, \tag{2.5}$$

and $[\![v]\!] := v$ on $E \subset \partial\Omega$. We assume that there is an orientation of the inner edges so that (2.5) is uniquely defined. This orientation is arbitrary and does not impact the results. We also define $\{v\}$, the average value of v on $E \in \mathcal{E}$, as

$$\{v\} := \frac{1}{2}(v|_K + v|_{K'})\,, \tag{2.6}$$

where K, K' are neighboring elements and on $E \subset \partial\Omega$, $\{v\} := v$. We define the broken products on $\mathscr{P}$ and $\partial\mathscr{P}$ as

$$(v,w)_{\mathscr{P}} := \sum_{K\in\mathscr{P}} (v,w)_K \quad \text{and} \quad \langle\mu, v\rangle_{\partial\mathscr{P}} := \sum_{K\in\mathscr{P}} \langle\mu, v\rangle_{\partial K}\,. \tag{2.7}$$

We recall from [29] that

$$\|\mu\|_\Lambda = \sup_{v\in V} \frac{\langle\mu, v\rangle_{\partial\mathscr{P}}}{\|v\|_V} \quad \text{for all } \mu \in \Lambda\,. \tag{2.8}$$

We also define the following norm over the space $L^2(\partial\mathscr{P})$

$$\|\mu\|_\star = \left(\sum_{K\in\mathscr{P}} \mathcal{H}_K\|\mu\|_{0,\partial K}^2 \right)^{1/2}. \tag{2.9}$$

We are ready to present a hybrid formulation for (2.1). Here we relax the continuity of u on the skeleton $\partial\mathscr{P}$ by introducing the Lagrange multiplier λ. The hybrid formulation reads: Find $(\lambda, u) \in \Lambda \times V$ such that

$$\begin{cases} (A\nabla u, \nabla v)_{\mathscr{P}} - \langle\lambda, v\rangle_{\partial\mathscr{P}} = (f, v)_{\mathscr{P}} & \text{for all } v \in V,\\ \langle\mu, u\rangle_{\partial\mathscr{P}} = \langle\mu, g\rangle_{\partial\Omega} & \text{for all } \mu \in \Lambda. \end{cases} \tag{2.10}$$

Observe that (2.10) is a saddle point problem wherein the exact solution u is sought in a space V larger than $H^1(\Omega)$. Nonetheless, the introduction of the Lagrange multiplier $\lambda \in \Lambda$, which ensures the weak continuity of u on $\mathscr{P}$, leads u to belong to $H^1(\Omega)$ and to satisfy the original formulation (2.1). These results were proved originally in [42] and extended in [9] to more general partitions $\mathscr{P}$.

2.3. **A characterization of the exact solution.** The exact solution of (2.1) can be characterized in terms of the solution to local and global problems. Following closely [4], we define the bounded mappings $\mathcal{T} \in \mathcal{L}(\Lambda, V)$ and $\hat{\mathcal{T}} \in \mathcal{L}(L^2(\Omega), V)$ as follows

- for all $\mu \in \Lambda$, $\mathcal{T}\mu\,|_K \in \tilde{V}$ is the unique solution of

$$\int_K A\nabla\mathcal{T}\mu\cdot\nabla v = \langle\mu, v\rangle_{\partial K} \quad \text{for all } v \in \tilde{V}\,,\ \forall\, K \in \mathscr{P}\,; \tag{2.11}$$

- for all $q \in L^2(\Omega)$, $\hat{\mathcal{T}} q\,|_K \in \tilde{V}$ is the unique solution of

$$\int_K A\nabla\hat{\mathcal{T}} q \cdot \nabla v = \int_K q\, v \quad \text{for all } v \in \tilde{V}\,,\ \forall\, K \in \mathscr{P}\,. \tag{2.12}$$

Hence, the solution of (2.1) can be written as

$$u = u_0 + \mathcal{T}\lambda + \hat{\mathcal{T}} f\,, \tag{2.13}$$

where $(\lambda, u_0) \in \Lambda \times V_0$ solves the following mixed problem

$$\begin{cases} \langle \mu, \mathcal{T}\lambda\rangle_{\partial\mathscr{P}} + \langle \mu, u_0\rangle_{\partial\mathscr{P}} = -\langle \mu, \hat{\mathcal{T}} f\rangle_{\partial\mathscr{P}} + \langle \mu, g\rangle_{\partial\Omega} & \text{for all } \mu \in \Lambda\,, \\ \langle \lambda, v_0\rangle_{\partial\mathscr{P}} = -(f, v_0)_{\mathscr{P}} & \text{for all } v_0 \in V_0\,. \end{cases} \tag{2.14}$$

The well-posedness of (2.14) was proved in [4, Section 3.1] for the partition of Ω into simplicial elements, and [9, Theorem 2.1] for more general cases.

3. The MHM method

This section presents the MHM method. Next, we introduce some notation needed to define the method in general polytopal meshes.

3.1. **Settings.** The MHM method uses a multi-level discretization starting from the first-level partition $\mathscr{P}$. Notably, each face $E \in \mathcal{E}$ and polytopal element $K \in \mathscr{P}$ may carry its own family of partitions in a way that each member is *a priori* independent of each other [29]. We start discretizing the set of faces $E \in \mathcal{E}$. For this, let $\{\mathcal{E}_H\}_{H>0}$ be a family of partitions of $\mathcal{E}$, for which each $E \in \mathcal{E}$ is split into faces F of diameter $H_F \le H := \max_{F\in\mathcal{E}_H} H_F$. We call $\mathcal{E}_H^K$ the collection of faces $F \in \mathcal{E}_H$ such that $F \subset \partial K$.

Assumption A: For each $K \in \mathscr{P}$, there exists $\{\Xi_H^K\}_{H>0}$ a shape-regular family of conforming simplicial partitions of K matching with $\{\mathcal{E}_H\}_{H>0}$, i.e., for each $F \in \mathcal{E}_H^K$ there exists an element $\kappa \in \Xi_H^K$ such that $\partial\kappa \cap \partial K = F$.

In addition, for each $K \in \mathscr{P}$, we introduce a shape regular family of simplicial triangulations $\{\mathscr{T}_h^K\}_{h>0}$ made up of simplices $T \in \mathscr{T}_h^K$ of diameter $h_T \le h := \max_{K\in\mathscr{P}} \max_{T\in\mathscr{T}_h^K} h_T$ (see Figure 1 for an illustration in two-dimensions). In each element $K \in \mathscr{P}$ the mesh $\mathscr{T}_h^K$ will be assumed to be a regular refinement of the triangulation Ξ_H^K. Let $\mathcal{F}_h^K$ denote the set of all facets of $\mathscr{T}_h^K$, and $\mathcal{F}_0^K \subset \mathcal{F}_h^K$ the set of facets internal to K. For $\mathfrak{f} \subset \partial T$, $h_\mathfrak{f}$ denotes its diameter. We note that every $\mathfrak{f} \subset \partial T \cap \partial K$ is included in one, and only one $F \in \mathcal{E}_H$.

For $k, \ell \ge 0$ we define the following finite element spaces associated to $\mathcal{E}_H$ and $\mathscr{T}_h^K$

$$\Lambda_H := \{\mu_H \in \Lambda : \mu_H|_F \in \mathbb{P}_\ell(F),\ \forall\, F \in \mathcal{E}_H\}\,, \tag{3.1}$$

$$V_h^k := \prod_{K\in\mathscr{P}} V_h^k(K)\,, \tag{3.2}$$

$$\tilde{V}_h := \prod_{K\in\mathscr{P}} \tilde{V}_h(K) \ \text{ where } \ \tilde{V}_h(K) := V_h^k(K) \cap L_0^2(K)\,, \tag{3.3}$$

where

$$V_h^k(K) := \{v_h \in C^0(K) \,:\, v_h|_T \in \mathbb{P}_k(T),\ \forall\, T \in \mathscr{T}_h^K\}\,, \quad \text{for } k \ge 1\,, \tag{3.4}$$

and $V_h^0(K) := \mathbb{P}_0(K)$.

Now, we introduce local projections onto more general piecewise polynomial spaces. For $K \in \mathscr{P}$, $m \ge 0$, we introduce the operator $\Pi_{K,m} : L^1(K) \to$

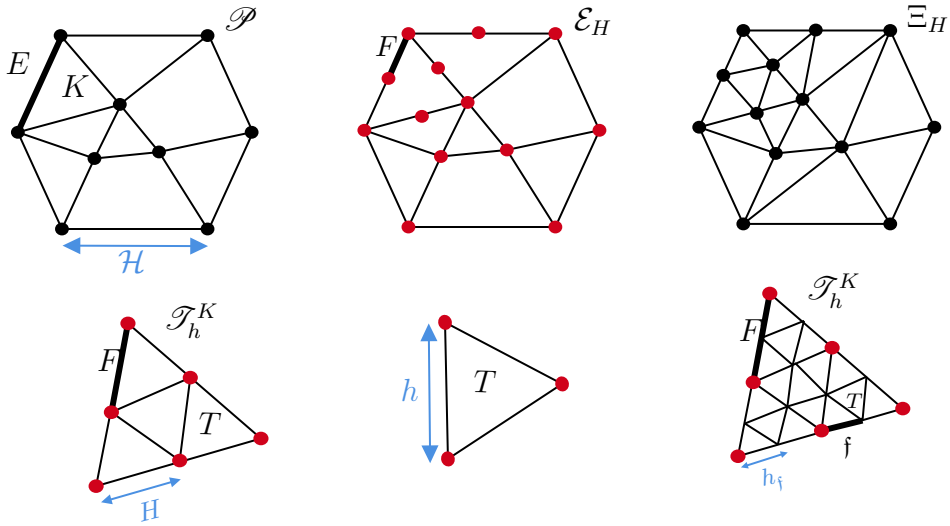

FIGURE 1. A polytopal domain $\mathscr{P}$ discretized with conforming elements K (upper left). The mesh $\mathcal{E}_H$ is defined over the skeleton of $\mathscr{P}$ (upper center). Ξ_H is a simplicial mesh (upper right) that matches $\mathcal{E}_H$. A minimal (bottom left) and a refined (bottom right) submesh in element K and a simplex T (bottom center). The black dots represent the degrees of freedom associated with Ξ_H and the red dots with the mesh skeleton.

$V_h^m(K)$ such that

$$\int_K \Pi_{K,m}(w)v = \int_K w\, v \quad \text{for all } v \in V_h^m(K)\,, \tag{3.5}$$

and the global projection $\Pi_{\Omega,m}(\cdot)$ such that $\Pi_{\Omega,m}(\cdot)|_K = \Pi_{K,m}(\cdot)$. Also, we define, for $T \in \mathscr{T}_h^K$, the operator $\boldsymbol{\Pi}_{T,m} : L^1(T)^d \to \mathbb{P}_m(T)^d$ as

$$\int_T \boldsymbol{\Pi}_{T,m}(\boldsymbol{w}) \cdot \boldsymbol{v} = \int_T \boldsymbol{w} \cdot \boldsymbol{v} \quad \text{for all } \boldsymbol{v} \in \mathbb{P}_m(T)^d\,. \tag{3.6}$$

In addition, for $F \in \mathcal{E}_H$, we define the projection operator $\Pi_{F,m} : L^1(F) \to \mathbb{P}_m(F)$ such that,

$$\int_F \Pi_{F,m}(\mu)\xi = \int_F \mu\, \xi \quad \text{for all } \xi \in \mathbb{P}_m(F)\,, \tag{3.7}$$

and the global projection operator $\Pi_{\mathcal{E},m}(\cdot)$ as $\Pi_{\mathcal{E},m}(\cdot)|_F = \Pi_{F,m}(\cdot)$.

3.2. **The MHM method.** Using the finite element spaces defined in (3.1)-(3.3), the discrete equivalents of the mappings $\mathcal{T}$ and $\hat{\mathcal{T}}$ defined in (2.11)-(2.12) read

- for all $\mu \in \Lambda$, $\mathcal{T}_h\mu \in \tilde{V}_h$ is the unique solution of

$$\int_K A\nabla\mathcal{T}_h\mu \cdot \nabla v_h = \langle \mu, v_h\rangle_{\partial K} \quad \text{for all } v_h \in \tilde{V}_h(K) \quad \text{and} \quad K \in \mathscr{P}\,; \tag{3.8}$$

- for all $q \in L^2(\Omega)$, $\hat{\mathcal{T}}_h q \in \tilde{V}_h$ is the unique solution of

$$\int_K A\nabla\hat{\mathcal{T}}_h q \cdot \nabla v_h = \int_K q\, v_h \quad \text{for all } v_h \in \tilde{V}_h(K) \quad \text{and} \quad K \in \mathscr{P}\,. \tag{3.9}$$

Using the discrete mappings (3.8)-(3.9), the discrete version of the problem (2.14) is: Find $(\lambda_H, u_0^h) \in \Lambda_H \times V_0$ such that

$$\begin{cases} \langle \mu_H, \mathcal{T}_h\lambda_H\rangle_{\partial\mathscr{P}} + \langle \mu_H, u_0^h\rangle_{\partial\mathscr{P}} = -\langle \mu_H, \hat{\mathcal{T}}_h f\rangle_{\partial\mathscr{P}} + \langle \mu_H, g\rangle_{\partial\Omega} & \text{for all } \mu_H \in \Lambda_H\,, \\ \langle \lambda_H, v_0\rangle_{\partial\mathscr{P}} = -(f, v_0)_{\mathscr{P}} & \text{for all } v_0 \in V_0\,. \end{cases} \tag{3.10}$$

The approximate solution is given by

$$u_{Hh} := u_0^h + \mathcal{T}_h \lambda_H + \hat{\mathcal{T}}_h f \,. \tag{3.11}$$

For the well-posedness of the MHM method, see [9, Theorem 2] for the two-dimensional case and [29, Theorem 4.4] for the three-dimensional case adapting it to the Darcy model.

Next, we present *a priori* error estimates for the MHM method. Hereafter, we denote by C a positive constant independent of mesh sizes, which may depend on physical coefficients $A_{\min}$, $A_{\max}$ and also on polynomial degrees ℓ and k.

Theorem 3.1. *Let us assume that u, solution of the hybrid formulation, belongs to $H^{k+1}(\mathscr{P})$ and $A\nabla u \in H^{\ell+1}(\mathscr{P}) \cap H(\mathrm{div};\Omega)$, with $\ell \geq 0$ and $k \geq \ell + d$. Then, there exists C such that*

$$\|u_0 - u_0^h\|_V + \|\lambda - \lambda_H\|_\Lambda \leq C \left(h^k |u|_{k+1,\mathscr{P}} + H^{\ell+1} |A\nabla u|_{\ell+1,\mathscr{P}} \right) .$$

In addition, the following error estimate holds for u_{Hh} as given in (3.11)

$$\|u - u_{Hh}\|_V \leq C \left(h^k |u|_{k+1,\mathscr{P}} + H^{\ell+1} |A\nabla u|_{\ell+1,\mathscr{P}} \right) .$$

Proof. For details, see [9, Theorem 3]. □

The simplest choice to approximate the exact flux $\boldsymbol{\sigma} = -A\nabla u$ is to adopt $-A\nabla u_{Hh}$, where u_{Hh} corresponds to the MHM solution obtained using a primal finite element method for local problems. However, $-A\nabla u_{Hh}$ is not necessarily in $H(\mathrm{div};\Omega)$, since its normal component over $E \in \mathcal{E}$ differs from λ_H. Furthermore, $-A\nabla u_{Hh}$ is not locally conservative. The approximated normal flow λ_H, in contrast, belongs to the desirable space $\Lambda_H \subset \Lambda$ and satisfies a locally conservative condition via (3.10). These reasons motivate the post-processing technique we present in the next section.

4. Post-processing for the dual variable for the MHM

To develop the flux recovery strategy from the solution of the MHM method (3.10), we use subspaces of finite dimension of $H(\mathrm{div};\Omega)$. Among the most renowned approximation spaces in the literature for $H(\mathrm{div};\Omega)$ are the Raviart-Thomas spaces. In this section, we propose to construct a $\boldsymbol{\sigma}_h$ in a way that its normal component is continuous on the interelement boundary, i.e., $\boldsymbol{\sigma}_h \in H(\mathrm{div};\Omega)$, through the definition of new local problems.

4.1. The Raviart-Thomas space.

Following [19, Section 3] we will build a Raviart-Thomas space in the submesh $\mathscr{T}_h^K$.

First, we introduce the local spaces. Given a simplex $T \subseteq \mathbb{R}^d$, the local Raviart-Thomas space of order $m \geq 0$ is defined by

$$\mathcal{RT}_m(T) = \mathbb{P}_m(T)^d + \boldsymbol{x}\mathbb{P}_m(T) \,. \tag{4.1}$$

The respective Raviart-Thomas local interpolation operator is defined as

$$\pi_T^{\mathcal{RT}_m} : H^s(T)^d \to \mathcal{RT}_m(T) \,, \tag{4.2}$$

with $s > 1/2$, where, for $\boldsymbol{v} \in H^s(T)^d$, $\pi_T^{\mathcal{RT}_m}\boldsymbol{v} \in \mathcal{RT}_m(T)$ is the only element of the local Raviart-Thomas space satisfying

$$\int_{\mathfrak{f}_i} (\pi_T^{\mathcal{RT}_m}\boldsymbol{v} \cdot \boldsymbol{n}_{\mathfrak{f}_i}^T)\mu = \int_{\mathfrak{f}_i} (\boldsymbol{v} \cdot \boldsymbol{n}_{\mathfrak{f}_i}^T)\mu \quad \text{for all } \mu \in \mathbb{P}_m(\mathfrak{f}_i) \,,\ i = 1, \cdots, d+1 \,, \tag{4.3}$$

and, if $m \geq 1$,

$$\int_T \pi_T^{\mathcal{RT}_m}\boldsymbol{v} \cdot \boldsymbol{\tau} = \int_T \boldsymbol{v} \cdot \boldsymbol{\tau} \quad \text{for all } \boldsymbol{\tau} \in \mathbb{P}_{m-1}(T)^d \,. \tag{4.4}$$

The Raviart-Thomas interpolation has an optimal-order error estimate, namely, there exist constants C depending on m, d, and the regularity constant of the mesh such that, for any $\boldsymbol{v} \in H^{m+1}(T)^d$,

$$\begin{aligned} \|\boldsymbol{v} - \pi_T^{\mathcal{RT}_m}\boldsymbol{v}\|_{0,T} &\leq C\, h_T^{m+1}|\boldsymbol{v}|_{m+1,T}\,, \\ \|\boldsymbol{v} - \pi_T^{\mathcal{RT}_m}\boldsymbol{v}\|_{0,\partial T} &\leq C\, h_T^{m+1/2}|\boldsymbol{v}|_{m+1,T}\,. \end{aligned} \tag{4.5}$$

Associated with $\mathscr{T}_h^K$ we introduce the global space over $K \in \mathscr{P}$

$$\mathcal{RT}_m(\mathscr{T}_h^K) = \{\boldsymbol{v} \in H(\mathrm{div};K) \,:\, \boldsymbol{v}|_T \in \mathcal{RT}_m(T)\,,\, \forall\, T \in \mathscr{T}_h^K\}\,. \tag{4.6}$$

An essential tool in error analysis is the operator

$$\pi_K^{\mathcal{RT}_m} : H(\mathrm{div};K) \cap \prod_{T\in\mathscr{T}_h^K} H^s(T)^d \to \mathcal{RT}_m(\mathscr{T}_h^K)\,,$$

with $s > 1/2$, defined by

$$\pi_K^{\mathcal{RT}_m}\boldsymbol{v}|_T = \pi_T^{\mathcal{RT}_m}\boldsymbol{v} \qquad \text{for all } T \in \mathscr{T}_h^K\,. \tag{4.7}$$

As a consequence of its definition, the operator $\pi_K^{\mathcal{RT}_m}$ satisfies

$$\int_K \nabla\cdot(\boldsymbol{v} - \pi_K^{\mathcal{RT}_m}\boldsymbol{v})q = 0\,,$$

for all $\boldsymbol{v} \in H(\mathrm{div};K) \cap \prod_{T\in\mathscr{T}_h^K} H^s(T)^d$ and all $q \in \{g \in L^2(K) : g|_T \in \mathbb{P}_m(T)\,, \forall\, T \in \mathscr{T}_h^K\}$, for every $K \in \mathscr{P}$. Moreover,

$$\nabla\cdot\mathcal{RT}_m(\mathscr{T}_h^K) = \{g \in L^2(K) : g|_T \in \mathbb{P}_m(T)\,,\, \forall\, T \in \mathscr{T}_h^K\}\,.$$

Also, in [22, Example 12.6], the following stability is proven: There exists $C > 0$, independent of $\mathcal{H}$, H, and h such that,

$$\|\boldsymbol{v}\|_{0,T} \leq C\left(\|\boldsymbol{\Pi}_{T,m-1}(\boldsymbol{v})\|_{0,T} + h_T^{1/2}\max_{\mathfrak{f}\subset\partial T}\|\boldsymbol{v}\cdot\boldsymbol{n}_{\mathfrak{f}}\|_{0,\mathfrak{f}}\right) \quad \forall\, \boldsymbol{v} \in \mathcal{RT}_m(T)\,, \tag{4.8}$$

where $\boldsymbol{\Pi}_{T,m-1}(\cdot)$ is defined in (3.6) with $m \geq 1$.

4.2. **Flux Recovery.** In this section we present the construction of the post-processed flux. Once the solution (λ_H, u_{Hh}) of the MHM method (3.10) is computed, we construct $\boldsymbol{\sigma}_h \in \mathcal{RT}_\ell(T)$ on each $T \in \mathscr{T}_h^K$, $\ell \geq 0$, as follows:

$$\begin{cases} \boldsymbol{\sigma}_h\cdot\boldsymbol{n}_{\mathfrak{f}} = -\lambda_H & \text{if } \mathfrak{f} \subset \partial T \cap \partial K\,, \\ \displaystyle\int_{\mathfrak{f}} (\boldsymbol{\sigma}_h\cdot\boldsymbol{n}_{\mathfrak{f}})\mu = \int_{\mathfrak{f}} -\{A\nabla u_{Hh}\}\cdot\boldsymbol{n}_{\mathfrak{f}}\,\mu & \text{for all } \mu \in \mathbb{P}_\ell(\mathfrak{f}),\ \text{if } \mathfrak{f} \in \mathcal{F}_0^K \cap \partial T\,, \\ \displaystyle\int_T \boldsymbol{\sigma}_h\cdot\boldsymbol{\tau} = \int_T -A\nabla u_{Hh}\cdot\boldsymbol{\tau} & \text{for all } \boldsymbol{\tau} \in \mathbb{P}_{\ell-1}(T)^d\,,\ (\ell \geq 1)\,, \end{cases} \tag{4.9}$$

where $\mathcal{F}_0^K \cap \partial T$ is the internal facet of T, $\boldsymbol{n}_{\mathfrak{f}}$ is a fixed unit normal to $\mathfrak{f}$ that points outward K if $\mathfrak{f} \subset \partial T \cap \partial K$. Note that, for $\ell = 0$, the third equation of (4.9) is not necessary.

Remark 4.1 (Generalizing existing techniques)**.** *The post-processing technique presented in* (4.9) *generalizes the ones proposed in [15] and [17] to the case of a multiscale method with a submesh. In fact, the techniques coincide in the case $\mathscr{P}$ is a simplicial triangulation, and as submesh we only take one element per each K, that is, $\mathscr{T}_h^K = \{K\}$ and $\mathcal{H} = H = h$. In such a case, since there is not a submesh, the second equation in* (4.9) *is no longer present.*

By construction, we immediately obtain the following two results.

Proposition 4.1. *The normal components of $\boldsymbol{\sigma}_h$ are continuous across the inter-element boundaries, i.e., we have $\boldsymbol{\sigma}_h \in H(\mathrm{div};\Omega)$.*

Proof. It follows from the first equation in (4.9) and the definition (2.5) that, for two elements K and K', if $\mathfrak{f} \subset \partial K \cap \partial T$ and $\mathfrak{f} \subset \partial K' \cap \partial T'$, for two adjacent elements T, T' such that $\mathfrak{f} = \partial T \cap \partial T'$, then

$$\left[\!\left[\boldsymbol{\sigma}_h \cdot \boldsymbol{n}_{\mathfrak{f}}\right]\!\right]|_{\mathfrak{f}} = -\lambda_H|_T - \lambda_H|_{T'} = 0\,.$$

On the other hand, if $\mathfrak{f} \in \mathcal{F}_0^K \cap \partial T$, let $\mu \in \mathbb{P}_\ell(\mathfrak{f})$, then, from the second equation in (4.9) and the definition (2.5),

$$\int_{\mathfrak{f}} \left[\!\left[\boldsymbol{\sigma}_h \cdot \boldsymbol{n}_{\mathfrak{f}}\right]\!\right] \mu = -\int_{\mathfrak{f}} \{A\nabla u_{Hh}\}|_T \cdot \boldsymbol{n}_{\mathfrak{f}}\, \mu + \int_{\mathfrak{f}} \{A\nabla u_{Hh}\}|_{T'} \cdot \boldsymbol{n}_{\mathfrak{f}}\, \mu = 0\,.$$

Hence, $\left[\!\left[\boldsymbol{\sigma}_h \cdot \boldsymbol{n}_{\mathfrak{f}}\right]\!\right]|_{\mathfrak{f}} = 0$, which implies that the normal component is continuous at the interelement boundaries, i.e., we have $\boldsymbol{\sigma}_h \in H(\mathrm{div};\Omega)$. □

The next result proves that the projection of the divergence of $\boldsymbol{\sigma}_h$ coincides with the projection of f onto the finite element space of continuous, piecewise polynomial functions in each K, relative to the submesh. The upshot is that $\boldsymbol{\sigma}_h$ is locally mass conservative in each $K \in \mathscr{P}$. It extends the proof of [44] to the MHM method which includes second-level submeshes.

Proposition 4.2. *The recovered flux $\boldsymbol{\sigma}_h$ defined in* (4.9) *satisfies*

$$\int_K \nabla \cdot \boldsymbol{\sigma}_h\, v = \int_K f\, v \qquad \text{for all } v \in V_h^\ell(K) \quad \text{and} \quad \ell \geq 0.$$

Proof. First, assume $\ell \geq 1$, and note that, for all $v \in V_h^\ell(K)$, using integration by parts and $v|_{\mathfrak{f}} \in \mathbb{P}_\ell(\mathfrak{f})$ for $\mathfrak{f} \subset \partial T$,

$$\int_K \nabla \cdot \boldsymbol{\sigma}_h\, v = \sum_{T\in\mathscr{T}_h^K} \int_T \nabla \cdot \boldsymbol{\sigma}_h\, v = \sum_{T\in\mathscr{T}_h^K} \left[-\int_T \boldsymbol{\sigma}_h \cdot \nabla v + \sum_{\mathfrak{f}\subset\partial T} \int_{\mathfrak{f}} \boldsymbol{\sigma}_h \cdot \boldsymbol{n}_{\mathfrak{f}}\, v \right].$$

Since $\nabla v|_T \in \mathbb{P}_{\ell-1}(T)^d$, we can use (4.9) to get

$$\int_K \nabla \cdot \boldsymbol{\sigma}_h\, v = \sum_{T\in\mathscr{T}_h^K} \left[\int_T A\nabla u_{Hh} \cdot \nabla v - \sum_{\mathfrak{f}\subset\partial T\cap\partial K} \int_{\mathfrak{f}} \lambda_H\, v \right] - \sum_{\mathfrak{f}\in\mathcal{F}_0^K\cap\partial T} \int_{\mathfrak{f}} \left[\!\left[\boldsymbol{\sigma}_h \cdot \boldsymbol{n}_{\mathfrak{f}}\right]\!\right]|_{\mathfrak{f}}\, v.$$

From Proposition 4.1, $\left[\!\left[\boldsymbol{\sigma}_h \cdot \boldsymbol{n}_{\mathfrak{f}}\right]\!\right]|_{\mathfrak{f}} = 0$, then, using (3.11), $v = v_0 + v^\perp$, (3.8)-(3.9) and (3.10),

$$\begin{aligned}\int_K \nabla \cdot \boldsymbol{\sigma}_h\, v &= \sum_{T\in\mathscr{T}_h^K} \int_T A\nabla u_{Hh} \cdot \nabla v - \int_{\partial K} \lambda_H\, v \\ &= \sum_{T\in\mathscr{T}_h^K} \int_T A\nabla(\mathcal{T}_h\lambda_H + \hat{\mathcal{T}}_h f) \cdot \nabla v^\perp - \int_{\partial K} \lambda_H\, v = \int_K f\, v\,.\end{aligned}$$

For the case $\ell = 0$, we follow analogous steps, and get

$$\int_K \nabla \cdot \boldsymbol{\sigma}_h = \sum_{T\in\mathscr{T}_h^K} \int_T \nabla \cdot \boldsymbol{\sigma}_h = \sum_{T\in\mathscr{T}_h^K} \sum_{\mathfrak{f}\subset\partial T} \int_{\mathfrak{f}} \boldsymbol{\sigma}_h \cdot \boldsymbol{n}_{\mathfrak{f}} = -\int_{\partial K} \lambda_H = \int_K f\,,$$

which finishes the proof. □

The next results shows the error estimate for $\nabla \cdot \boldsymbol{\sigma}_h$ in the $L^2(\Omega)-$norm assuming $f \in H^{\ell+1}(\mathscr{P})$.

Theorem 4.1. *Let $\ell \geq 0$ and $k \geq \ell + d$ be the polynomial orders of the MHM method* (3.10)*. Assume that the exact solution of* (2.1) *satisfies $f \in H^{\ell+1}(\mathscr{P})$. Then the approximated flux $\boldsymbol{\sigma}_h \in H(\mathrm{div};\Omega)$ defined in* (4.9) *satisfies*

$$\|\nabla \cdot \boldsymbol{\sigma} - \Pi_{\Omega,\ell}(\nabla \cdot \boldsymbol{\sigma}_h)\|_{0,\Omega} \leq C h^{\ell+1} |f|_{\ell+1,\mathscr{P}}\,.$$

Proof. It is not difficult to realize that Proposition 4.2 implies that $\Pi_{\Omega,\ell}(\nabla\cdot\boldsymbol{\sigma}_h)=\Pi_{\Omega,\ell}(\nabla\cdot\boldsymbol{\sigma})=\Pi_{\Omega,\ell}(f)$. Then, using standard finite element approximation results (e.g. [22, Corollary 19.8]) the following holds

$$\|\nabla\cdot\boldsymbol{\sigma}-\Pi_{\Omega,\ell}(\nabla\cdot\boldsymbol{\sigma}_h)\|_{0,\Omega}=\|f-\Pi_{\Omega,\ell}(f)\|_{0,\Omega}\leq Ch^{\ell+1}|f|_{\ell+1,\mathscr{P}}\,,$$

which finishes the proof. □

Remark 4.2 (The one-element submesh case)**.** *In the case $\mathscr{P}$ is a simplicial partition and the submesh contains only one element, i.e. $\mathscr{T}_h^K=\{K\}$ and $h=\mathcal{H}$, the reconstructed flux $\boldsymbol{\sigma}_h\in H(\mathrm{div};\Omega)$ defined in* (4.9) *satisfies $\nabla\cdot\boldsymbol{\sigma}_h=\Pi_{K,\ell}(f)$, for $\ell\geq 0$, from Proposition 4.2. Hence, it follows*

$$\|\nabla\cdot\boldsymbol{\sigma}-\nabla\cdot\boldsymbol{\sigma}_h\|_{0,\Omega}\;\leq\;C\,\mathcal{H}^{\ell+1}|f|_{\ell+1,\mathscr{P}}\,,$$

and we recover the result presented in [17].

The upcoming lemma holds significance about the error estimates for the post-processed dual variable.

Lemma 4.1. *Let $\mu\in\Lambda_H$. Then*

$$\|\mu\|_\star\leq C\,\|\mu\|_\Lambda\,. \tag{4.10}$$

Proof. Note that, for $\mu\in\Lambda_H$, there exists $\tilde{\boldsymbol{\tau}}_H\in\mathcal{RT}_\ell(\Xi_H)$ such that $\tilde{\boldsymbol{\tau}}_H\cdot\boldsymbol{n}^K=\mu$ on every $F\in\mathcal{E}_H$. Thus, using a local trace and inverse inequalities (c.f. [22, Lemma 12.8]), for a constant C independent of H, h and $\mathcal{H}$,

$$\|\mu\|_\star^2=\sum_{K\in\mathscr{P}}\mathcal{H}_K\|\tilde{\boldsymbol{\tau}}_H\cdot\boldsymbol{n}^K\|_{0,\partial K}^2\leq C\sum_{K\in\mathscr{P}}\|\tilde{\boldsymbol{\tau}}_H\|_{0,K}^2\leq C\,\|\tilde{\boldsymbol{\tau}}_H\|_{\mathrm{div},\Omega}^2\leq C\,\|\mu\|_\Lambda^2\,,$$

where we used the fact that $\boldsymbol{n}^K$ is the unit outward normal to ∂K, (2.4), and (2.3). □

The next result is an error estimate for the $L^2(\Omega)-$norm of $\boldsymbol{\sigma}_h$. To this end, we assume from now on that $A|_T$ is a polynomial for all $T\in\mathscr{T}_h^K$ and $K\in\mathscr{P}$. This assumption is not restrictive, as the polynomial degree can be chosen arbitrarily. However, in this case, the constants C may depend on the polynomial degree of $A|_T$, for all $T\in\mathscr{T}_h^K$.

Theorem 4.2. *Let $\ell\geq 0$ and $k\geq\ell+d$ be the polynomial orders of the MHM method* (3.10)*. Assume that the exact solution of* (2.1) *satisfies $u\in H^{k+1}(\mathscr{P})$, $A\nabla u\in H^{\ell+1}(\mathscr{P})\cap H(\mathrm{div};\Omega)$. Then the approximated flux $\boldsymbol{\sigma}_h\in H(\mathrm{div};\Omega)$ defined in* (4.9) *satisfies*

$$\|\boldsymbol{\sigma}-\boldsymbol{\sigma}_h\|_{0,\Omega}\leq C\,\left(h^k|u|_{k+1,\mathscr{P}}+H^{\ell+1}|A\nabla u|_{\ell+1,\mathscr{P}}+h^{\ell+1}|A\nabla u|_{\ell+1,\mathscr{P}}\right)\,.$$

Moreover, assuming that $f\in H^{k+1}(\mathscr{P})$ and that there exist C_1,C_2, two positive constants independent of mesh parameters such that $C_1h\leq H\leq C_2\,h_{min}$, where

$$h_{min}:=\min\{h_T\,,\,\forall\,T\in\mathscr{T}_h^K,K\in\mathscr{P}\}\,,$$

we have

$$\|\nabla\cdot\boldsymbol{\sigma}-\nabla\cdot\boldsymbol{\sigma}_h\|_{0,\Omega}\leq C\left(h^{k-1}|u|_{k+1,\mathscr{P}}+(H^\ell+h^\ell)|A\nabla u|_{\ell+1,\mathscr{P}}+h^{k+1}|f|_{k+1,\mathscr{P}}\right).$$

Proof. The triangle inequality gives,

$$\|\boldsymbol{\sigma}-\boldsymbol{\sigma}_h\|_{0,\Omega}\leq\underbrace{\left\{\sum_{K\in\mathscr{P}}\|\boldsymbol{\sigma}-\pi_K^{\mathcal{RT}_\ell}\boldsymbol{\sigma}\|_{0,K}^2\right\}^{1/2}}_{(i)}+\underbrace{\left\{\sum_{K\in\mathscr{P}}\|\pi_K^{\mathcal{RT}_\ell}\boldsymbol{\sigma}-\boldsymbol{\sigma}_h\|_{0,K}^2\right\}^{1/2}}_{(ii)}\,.$$

For (i), from (4.5), we have that

$$\left\{\sum_{K\in\mathscr{P}}\|\boldsymbol{\sigma}-\pi_K^{\mathcal{RT}_\ell}\boldsymbol{\sigma}\|_{0,K}^2\right\}^{1/2}\leq Ch^{\ell+1}|A\nabla u|_{\ell+1,\mathscr{P}}\,. \tag{4.11}$$

Now we need to estimate (ii). We shall apply now (4.8) to $\boldsymbol{v}_h := (\pi_K^{\mathcal{RT}_\ell}\boldsymbol{\sigma} - \boldsymbol{\sigma}_h)|_T \in \mathcal{RT}_\ell(T)$. For all $T \in \mathscr{T}_h^K$ and $\boldsymbol{v}_h \in \mathcal{RT}_\ell(T)$,

$$\begin{aligned}\sum_{T\in\mathscr{T}_h^K} \|\boldsymbol{v}_h\|_{0,T}^2 \leq C \sum_{T\in\mathscr{T}_h^K} \Big(&\|\boldsymbol{\Pi}_{T,\ell-1}(\boldsymbol{v}_h)\|_{0,T}^2 + \\ &h_T \left\{ \sum_{\mathfrak{f}\subset\partial T\cap\partial K} \|\boldsymbol{v}_h\cdot\boldsymbol{n}_\mathfrak{f}\|_{0,\mathfrak{f}}^2 + \sum_{\mathfrak{f}\in\mathcal{F}_0^K\cap\partial T} \|\boldsymbol{v}_h\cdot\boldsymbol{n}_\mathfrak{f}\|_{0,\mathfrak{f}}^2 \right\} \Big) \\ = C \sum_{T\in\mathscr{T}_h^K} \big((a) + h_T\{(b)+(c)\} \big)&. \end{aligned} \tag{4.12}$$

Let $T \in \mathscr{T}_h^K$, and let us bound (a). For $\boldsymbol{\tau} \in \mathbb{P}_{\ell-1}(T)^d$, using $\boldsymbol{\sigma} = -A\nabla u$ and the third equation in (4.9),

$$\int_T \boldsymbol{\Pi}_{T,\ell-1}(\boldsymbol{v}_h)\cdot\boldsymbol{\tau} = \int_T (\pi_T^{\mathcal{RT}_\ell}\boldsymbol{\sigma} - \boldsymbol{\sigma}_h)\cdot\boldsymbol{\tau} = \int_T A\nabla(u_{Hh}-u)\cdot\boldsymbol{\tau}\,.$$

Taking $\boldsymbol{\tau} = \boldsymbol{\Pi}_{T,\ell-1}(\boldsymbol{v}_h)$ and using the Cauchy-Schwarz inequality, we get

$$(a) = \|\boldsymbol{\Pi}_{T,\ell-1}(\boldsymbol{v}_h)\|_{0,T}^2 \leq \|A\nabla(u_{Hh}-u)\|_{0,T}\|\boldsymbol{\Pi}_{T,\ell-1}(\boldsymbol{v}_h)\|_{0,T}\,,$$

which implies that

$$\|\boldsymbol{\Pi}_{T,\ell-1}(\boldsymbol{v}_h)\|_{0,T} \leq \|A\nabla(u_{Hh}-u)\|_{0,T}\,. \tag{4.13}$$

Now we only need to find estimates for (b) and (c). For (c), let $\mathfrak{f} \in \mathcal{F}_0^K$ s.t. $\mathfrak{f} \subset \partial T \cap \partial T'$. For all $\mu \in \mathbb{P}_\ell(\mathfrak{f})$, a fixed $\boldsymbol{n}_\mathfrak{f}$, using (4.9), (2.6) and properties of $\pi_T^{\mathcal{RT}_\ell}$, we get

$$\begin{aligned}\int_\mathfrak{f} \boldsymbol{v}_h\cdot\boldsymbol{n}_\mathfrak{f}\,\mu &= \int_\mathfrak{f} \pi_T^{\mathcal{RT}_\ell}\boldsymbol{\sigma}\cdot\boldsymbol{n}_\mathfrak{f}\,\mu + \int_\mathfrak{f}\{A\nabla u_{Hh}\}\cdot\boldsymbol{n}_\mathfrak{f}\,\mu \\ &= \int_\mathfrak{f} \pi_T^{\mathcal{RT}_\ell}\boldsymbol{\sigma}\cdot\boldsymbol{n}_\mathfrak{f}\,\mu + \int_\mathfrak{f} \frac{1}{2}(A\nabla u_{Hh}|_T + A\nabla u_{Hh}|_{T'})\cdot\boldsymbol{n}_\mathfrak{f}\,\mu \\ &= \sum_{T\in\omega_\mathfrak{f}} \frac{1}{2}\int_\mathfrak{f} \Big(A\nabla u_{Hh}|_T + \pi_T^{\mathcal{RT}_\ell}\boldsymbol{\sigma} \Big)\cdot\boldsymbol{n}_\mathfrak{f}\,\mu\,.\end{aligned}$$

Then, taking $\mu = \boldsymbol{v}_h\cdot\boldsymbol{n}_\mathfrak{f}$, from the Cauchy-Schwarz inequality,

$$(c) = \|\boldsymbol{v}_h\cdot\boldsymbol{n}_\mathfrak{f}\|_{0,\mathfrak{f}}^2 \leq \frac{1}{2}\sum_{T\in\omega_\mathfrak{f}} \|(A\nabla u_{Hh}|_T + \pi_T^{\mathcal{RT}_\ell}\boldsymbol{\sigma})\cdot\boldsymbol{n}_\mathfrak{f}\|_{0,\mathfrak{f}}\|\boldsymbol{v}_h\cdot\boldsymbol{n}_\mathfrak{f}\|_{0,\mathfrak{f}}\,,$$

and, from Theorem A.2,

$$\|(A\nabla u_{Hh}|_T + \pi_T^{\mathcal{RT}_\ell}\boldsymbol{\sigma})\cdot\boldsymbol{n}_\mathfrak{f}\|_{0,\mathfrak{f}} \leq C\left(h_T^{-1/2}|u-u_{Hh}|_{1,T} + \|\pi_T^{\mathcal{RT}_\ell}\boldsymbol{\sigma} - \boldsymbol{\sigma}\|_{0,\partial T}\right).$$

Summing up over all internal facets implies that,

$$\sum_{\mathfrak{f}\in\mathcal{F}_0^K\cap\partial T} \|\boldsymbol{v}_h\cdot\boldsymbol{n}_\mathfrak{f}\|_{0,\mathfrak{f}}^2 \leq C \sum_{\mathfrak{f}\in\mathcal{F}_0^K\cap\partial T}\sum_{T'\in\omega_\mathfrak{f}} \left(h_{T'}^{-1}|u-u_{Hh}|_{1,T'}^2 + \|\pi_{T'}^{\mathcal{RT}_\ell}\boldsymbol{\sigma} - \boldsymbol{\sigma}\|_{0,\partial T'}^2\right). \tag{4.14}$$

On the other hand, for (b), first note that $A\nabla u\,|_K \in H^{\ell+1}(K)$ implies $\lambda \in L^2(\partial K)$ for all $K \in \mathscr{P}$. Next, if $\mathfrak{f} \subset \partial T \cap \partial K$, for all $\mu \in \mathbb{P}_\ell(\mathfrak{f})$, from the first

equation in (4.9) and the definition of $\Pi_{\mathcal{E},\ell}(\cdot)$, we get

$$\begin{aligned}\sum_{\mathfrak{f}\subset\partial T\cap\partial K}\int_{\mathfrak{f}}\boldsymbol{v}_h\cdot\boldsymbol{n}_{\mathfrak{f}}\,\mu &= \sum_{\mathfrak{f}\subset\partial T\cap\partial K}\int_{\mathfrak{f}}(\boldsymbol{\sigma}\cdot\boldsymbol{n}_{\mathfrak{f}}-\boldsymbol{\sigma}_h\cdot\boldsymbol{n}_{\mathfrak{f}})\mu\\ &= \int_{\partial K}(-\lambda+\lambda_H)\mu\\ &= \int_{\partial K}(-\Pi_{\mathcal{E},\ell}(\lambda)+\lambda_H)\mu\,.\end{aligned}$$

Again, taking $\mu=\boldsymbol{v}_h\cdot\boldsymbol{n}_{\mathfrak{f}}$, from the Cauchy-Schwarz inequality,

$$(b)=\sum_{\mathfrak{f}\subset\partial T\cap\partial K}\|\boldsymbol{v}_h\cdot\boldsymbol{n}_{\mathfrak{f}}\|^2_{0,\mathfrak{f}}\le\|\Pi_{\mathcal{E},\ell}(\lambda)-\lambda_H\|_{0,\partial K}\left\{\sum_{\mathfrak{f}\subset\partial T\cap\partial K}\|\boldsymbol{v}_h\cdot\boldsymbol{n}_{\mathfrak{f}}\|^2_{0,\mathfrak{f}}\right\}^{1/2},$$

which implies that

$$\left\{\sum_{\mathfrak{f}\subset\partial T\cap\partial K}\|\boldsymbol{v}_h\cdot\boldsymbol{n}_{\mathfrak{f}}\|^2_{0,\mathfrak{f}}\right\}^{1/2}\le\|\Pi_{\mathcal{E},\ell}(\lambda)-\lambda_H\|_{0,\partial K}\,. \tag{4.15}$$

Then, applying (4.13)-(4.15) to (4.12) we obtain

$$\begin{aligned}\sum_{T\in\mathscr{T}_h^K}\|\boldsymbol{v}_h\|^2_{0,T}\le C\Big[&\sum_{T\in\mathscr{T}_h^K}\Big(\|A\nabla(u_{Hh}-u)\|^2_{0,T}+h_T\|\Pi_{\mathcal{E},\ell}(\lambda)-\lambda_H\|^2_{0,\partial K}\\ &+\sum_{\mathfrak{f}\in\mathcal{F}_0^K\cap\partial T}\sum_{T'\in\omega_{\mathfrak{f}}}\|A\nabla(u-u_{Hh})\|^2_{0,T'}+h_{T'}\|\pi_{T'}^{\mathcal{RT}_\ell}\boldsymbol{\sigma}-\boldsymbol{\sigma}\|^2_{0,\partial T'}\Big)\Big]\\ \le C\sum_{T\in\mathscr{T}_h^K}&\Big\{\|u-u_{Hh}\|^2_{1,T}+h_T\Big(\|\Pi_{\mathcal{E},\ell}(\lambda)-\lambda_H\|^2_{0,\partial K}+\|\pi_T^{\mathcal{RT}_\ell}\boldsymbol{\sigma}-\boldsymbol{\sigma}\|^2_{0,\partial T}\Big)\Big\}\,.\end{aligned} \tag{4.16}$$

Finally, adding over $K\in\mathscr{P}$ and using (2.9) and (4.5), we get

$$\|\boldsymbol{v}_h\|_{0,\mathscr{P}}\le C\,\|u-u_{Hh}\|_V+\|\Pi_{\mathcal{E},\ell}(\lambda)-\lambda_H\|_\star+h^{\ell+1}|A\nabla u|_{\ell+1,\mathscr{P}}\,.$$

Now, we only need to find an estimate for $\|\Pi_{\mathcal{E},\ell}(\lambda)-\lambda_H\|_\star$. From Lemma 4.1 we have that

$$\|\Pi_{\mathcal{E},\ell}(\lambda)-\lambda_H\|_\star\le C\,\|\Pi_{\mathcal{E},\ell}(\lambda)-\lambda_H\|_\Lambda\le C\,\left(\|\Pi_{\mathcal{E},\ell}(\lambda)-\lambda\|_\Lambda+\|\lambda-\lambda_H\|_\Lambda\right),$$

where we used the fact that $\Pi_{\mathcal{E},\ell}(\lambda)\in\Lambda_H$ and $\lambda_H\in\Lambda_H$. Then, from Theorem 3.1 and global interpolation (c.f. [22, Section 19.3]),

$$\|\lambda-\lambda_H\|_\star\le C(h^k|u|_{k+1,\mathscr{P}}+H^{\ell+1}|A\nabla u|_{\ell+1,\mathscr{P}})\,.$$

We then arrive that, the estimate for (ii) is,

$$\left\{\sum_{K\in\mathscr{P}}\|\pi_K^{\mathcal{RT}_\ell}\boldsymbol{\sigma}-\boldsymbol{\sigma}_h\|^2_{0,K}\right\}^{1/2}\le C\,\left(h^k|u|_{k+1,\mathscr{P}}+(H^{\ell+1}+h^{\ell+1})|A\nabla u|_{\ell+1,\mathscr{P}}\right). \tag{4.17}$$

From (i) and (ii) we have

$$\|\boldsymbol{\sigma}-\boldsymbol{\sigma}_h\|_{0,\Omega}\le C\,\left(h^k|u|_{k+1,\mathscr{P}}+H^{\ell+1}|A\nabla u|_{\ell+1,\mathscr{P}}+h^{\ell+1}|A\nabla u|_{\ell+1,\mathscr{P}}\right). \tag{4.18}$$

Next, using the triangle inequality, an inverse inequality in each T, and (4.17), we arrive at

$$\begin{aligned}
\|\nabla\cdot\boldsymbol{\sigma}-\nabla\cdot\boldsymbol{\sigma}_h\|_{0,\Omega} &\leq \left\{\sum_{K\in\mathscr{P}}\sum_{T\in\mathscr{T}_h^K}\|\nabla\cdot\boldsymbol{\sigma}-\nabla\cdot\pi_T^{\mathcal{RT}_\ell}\boldsymbol{\sigma}\|_{0,T}^2\right\}^{1/2}\\
&\quad+\left\{\sum_{K\in\mathscr{P}}\sum_{T\in\mathscr{T}_h^K}\|\nabla\cdot\pi_T^{\mathcal{RT}_\ell}\boldsymbol{\sigma}-\nabla\cdot\boldsymbol{\sigma}_h\|_{0,T}^2\right\}^{1/2}\\
&\leq C\left(h^{k+1}|f|_{k+1,\mathscr{P}}+\left\{\sum_{K\in\mathscr{P}}\sum_{T\in\mathscr{T}_h^K}h_T^{-2}\|\pi_T^{\mathcal{RT}_\ell}\boldsymbol{\sigma}-\boldsymbol{\sigma}_h\|_{0,T}^2\right\}^{1/2}\right)\\
&\leq C\left(h^{k+1}|f|_{k+1,\mathscr{P}}+H^{-1}\left\{\sum_{K\in\mathscr{P}}\|\pi_K^{\mathcal{RT}_\ell}\boldsymbol{\sigma}-\boldsymbol{\sigma}_h\|_{0,K}^2\right\}^{1/2}\right)\\
&\leq C\left(h^{k+1}|f|_{k+1,\mathscr{P}}+h^{k-1}|u|_{k+1,\mathscr{P}}+(H^\ell+h^\ell)|A\nabla u|_{\ell+1,\mathscr{P}}\right),
\end{aligned}$$

which finishes the proof. □

5. A fully computable *a posteriori* error bound

In this section, we propose and analyze a computable and efficient procedure for *a posteriori* error estimation for the provided approximate solutions. To analyze the *a posteriori* estimator we assume the following extra conditions.

Assumption B: The union $\mathscr{T}_h := \bigcup_{K\in\mathscr{P}}\mathscr{T}_h^K$ is a conforming triangulation of $\overline{\Omega}$.

Assumption C: $\mathscr{P}$ consists of convex polytopes K.

Remark 5.1 (An alternative flux recovery)**.** *Assumption B allows us to modify the flux recovery $\boldsymbol{\sigma}_h$ slightly. In fact, since the union of the local triangulations $\mathscr{T}_h^K$ defines a conforming triangulation in the whole domain, we can modify the definition of $\boldsymbol{\sigma}_h$ in the following way: For $\ell\leq m\leq k$, with $k\geq\ell+d$, $\boldsymbol{\sigma}_h\in\mathcal{RT}_m(T)$ is defined as,*

(5.1)
$$\begin{cases}
\displaystyle\int_{\mathfrak{f}}(\boldsymbol{\sigma}_h\cdot\boldsymbol{n}_{\mathfrak{f}})\mu=\int_{\mathfrak{f}}-\lambda_H\,\mu & \text{for all } \mu\in\mathbb{P}_m(\mathfrak{f}),\ \text{if } \mathfrak{f}\subset\partial K\cap\partial T,\\
\displaystyle\int_{\mathfrak{f}}(\boldsymbol{\sigma}_h\cdot\boldsymbol{n}_{\mathfrak{f}})\mu=\int_{\mathfrak{f}}-\{A\nabla u_{Hh}\}\cdot\boldsymbol{n}_{\mathfrak{f}}\,\mu & \text{for all } \mu\in\mathbb{P}_m(\mathfrak{f}),\ \text{if } \mathfrak{f}\in\mathcal{F}_0^K\cap\partial T,\\
\displaystyle\int_T\boldsymbol{\sigma}_h\cdot\boldsymbol{\tau}=\int_T-A\nabla u_{Hh}\cdot\boldsymbol{\tau} & \text{for all } \boldsymbol{\tau}\in\mathbb{P}_{m-1}(T)^d,\ (m\geq 1).
\end{cases}$$

This definition extends (4.9) *allowing us to recover the flux $\boldsymbol{\sigma}_h$ onto a higher-order polynomial degree. Theorems 4.2 and 4.1 also apply, and we can, in particular, prove*

$$\|\nabla\cdot\boldsymbol{\sigma}-\Pi_{\Omega,m}(\nabla\cdot\boldsymbol{\sigma}_h)\|_{0,\Omega}\leq Ch^{m+1}|f|_{m+1,\mathscr{P}},$$

where $C>0$ is a constant independent of h.

Now we introduce the Oswald interpolation operator $I_{OS}: V_h^k \to V_h^k \cap H_0^1(\Omega)$ [39, 27] as follows: for $\varphi_h \in V_h^k$ and a Lagrange node $V \in \Omega$,

$$I_{OS}(\varphi_h)(V) = \frac{1}{\#\widehat{\mathscr{T}_V}} \sum_{T \in \widehat{\mathscr{T}_V}} \varphi_h|_T(V)\,, \tag{5.2}$$

where $\widehat{\mathscr{T}_V} := \{T \in \mathscr{T}_h \,:\, V \in T\}$ and $\#\widehat{\mathscr{T}_V}$ denotes the cardinality of the set $\widehat{\mathscr{T}_V}$. The Oswald operator is computationally efficient, requiring only local averaging at shared Lagrange nodes. It smooths out flux jumps at element interfaces, ensuring a stable and robust recovered potential in $H^1(\Omega)$ with respect to mesh parameters. There are reconstruction alternatives that also ensure robustness with respect to the degree of the polynomial by post-processing the primal variable on element patches (see, for example, [24, 14]).

With these ingredients, we present the main result on the *a posteriori* estimator following the steps of [24, Theorem 3.3].

Theorem 5.1. *Assume $\ell \geq 0$, $k \geq \ell + d$ and $\ell \leq m \leq k$. Let $u \in H_0^1(\Omega)$ be the solution of (2.1), and u_{Hh} be the solution of the MHM method (3.10). Let $\boldsymbol{\sigma}_h$ be the equilibrated flux reconstruction defined through (5.1), and define the local quantities*

$$\eta_{1,K} := \|A\nabla u_{Hh} + \boldsymbol{\sigma}_h\|_{0,K}\,, \tag{5.3}$$

$$\eta_{2,K} = \|A^{1/2}\nabla(u_{Hh} - I_{OS}(u_{Hh}))\|_{0,K}\,, \tag{5.4}$$

and

$$\eta_{3,K} = \frac{\mathcal{H}_K}{\pi}\|\Pi_{K,m}(\nabla\cdot\boldsymbol{\sigma}_h) - \nabla\cdot\boldsymbol{\sigma}_h\|_{0,K}\,. \tag{5.5}$$

Then, the following upper bound holds

$$\|A^{1/2}\nabla(u - u_{Hh})\|_{0,\mathscr{P}}^2 \leq \eta^2 := \sum_{K\in\mathscr{P}}(\eta_{1,K} + \eta_{osc,K}^f + \eta_{3,K})^2 + \sum_{K\in\mathscr{P}}\eta_{2,K}^2\,, \tag{5.6}$$

where for any $K \in \mathscr{P}$, $\eta_{osc,K}^f$ is the oscillation term defined by

$$\eta_{osc,K}^f := \frac{\mathcal{H}_K}{\pi}\|f - \Pi_{K,m}(f)\|_{0,K}\,. \tag{5.7}$$

In addition, assuming $\boldsymbol{\sigma} := -A\nabla u \in H(\mathrm{div};\Omega)\cap H^s(\Omega)$, $s > 1/2$, the following local lower bounds hold

(5.8)

$$\eta_{1,K} \leq C\,\|A^{1/2}\nabla(u - u_{Hh})\|_{0,K} + \eta_{ho,K}^{\boldsymbol{\sigma}} + \mathcal{H}_K^{1/2}\|\Pi_{\mathcal{E},m}(\lambda) - \lambda_H\|_{0,\partial K}\,,$$

$$\eta_{2,K} \leq C\left\{\sum_{F\in\mathcal{E}_H^K}\frac{H_F}{\min\limits_{\mathfrak{f}\subset F} h_{\mathfrak{f}}}\|A^{1/2}\nabla(u - u_{Hh})\|_{0,\omega_K^F}^2\right\}^{1/2},$$

$$\eta_{3,K} \leq C\left(\sum_{T\in\mathscr{T}_h^K}\frac{\mathcal{H}_K^2}{h_T^2}\left\{\|A^{1/2}\nabla(u - u_{Hh})\|_{0,T}^2 + h_T\|\Pi_{\mathcal{E},m}(\lambda) - \lambda_H\|_{0,\partial K}^2\right\}\right)^{1/2} + C\,\eta_{osc,K}^f\,,$$

where $\eta_{ho,K}^{\boldsymbol{\sigma}}$ is the high-order term

$$\eta_{ho,K}^{\boldsymbol{\sigma}} := \|\boldsymbol{\sigma} - \pi_K^{\mathcal{RT}_m}\boldsymbol{\sigma}\|_{0,K}\,, \tag{5.9}$$

and $\omega_K^F := \{\kappa \in \Xi_H^K \,:\, \kappa \subset K \quad or \quad \kappa \cap K = F \in \mathcal{E}_H\}$. Moreover, if there exist C such that $H_F \leq C\,h_{\mathfrak{f}}$ and $\mathcal{H}_K \leq C\,h_T$ for all $F \in \mathcal{E}_H^K$, $\mathfrak{f} \in \mathcal{F}_h^K \cap \partial K$,

$T \in \mathscr{T}_h^K$ and $K \in \mathscr{P}$, the following global lower bound holds

$$\eta^2 \leq C \Big(\|A^{1/2}\nabla(u_{Hh} - u)\|_{0,\mathscr{P}}^2 + \|\Pi_{\mathcal{E},m}(\lambda) - \lambda_H\|_{\Lambda}^2 + \sum_{K\in\mathscr{P}} (\eta_{ho,K}^{\boldsymbol{\sigma}})^2 + \sum_{K\in\mathscr{P}} (\eta_{osc,K}^{f})^2 \Big). \tag{5.10}$$

Remark 5.2 (High-order and oscillation terms)**.** *It is important to mention that, since we allow $m \geq \ell$, then $\eta_{ho,K}^{\boldsymbol{\sigma}}$ and $\eta_{osc,K}^{f}$ are indeed high-order and oscillation terms, respectively, for $m > \ell$.*

Proof. Let $s \in H_0^1(\Omega)$ be the unique solution of

$$(A\nabla s, \nabla v)_{\mathscr{P}} = (A\nabla u_{Hh}, \nabla v)_{\mathscr{P}} \quad \forall\, v \in H_0^1(\Omega)\,. \tag{5.11}$$

Then from the Pythagorean equality

$$\|A^{1/2}\nabla(u - u_{Hh})\|_{0,\Omega}^2 = \|A^{1/2}\nabla(u - s)\|_{0,\mathscr{P}}^2 + \|A^{1/2}\nabla(s - u_{Hh})\|_{0,\mathscr{P}}^2\,. \tag{5.12}$$

Moreover,

$$\|A^{1/2}\nabla(s - u_{Hh})\|_{0,\mathscr{P}}^2 = \min_{w\in H_0^1(\Omega)} \|A^{1/2}\nabla(w - u_{Hh})\|_{0,\mathscr{P}}^2\,. \tag{5.13}$$

It follows from (5.13) that, for $w = I_{OS}(u_{Hh})$, we have the bound

$$\|A^{1/2}\nabla(s - u_{Hh})\|_{0,\mathscr{P}}^2 \leq \|A^{1/2}\nabla(u_{Hh} - I_{OS}(u_{Hh}))\|_{0,\mathscr{P}}^2 = \sum_{K\in\mathscr{P}} \eta_{2,K}^2\,. \tag{5.14}$$

For the first term in (5.12), we note that $u - s \in H_0^1(\Omega)$. Thus, from the definition of $s \in H_0^1(\Omega)$ and the energy norm for a function in $H_0^1(\Omega)$,

$$\begin{aligned} \|A^{1/2}\nabla(u - s)\|_{0,\Omega}^2 &= \sup_{\substack{\varphi\in H_0^1(\Omega)\\ \|\nabla\varphi\|_{0,\Omega}=1}} (A\nabla(u - s), \nabla\varphi)_{\mathscr{P}} \\ &= \sup_{\substack{\varphi\in H_0^1(\Omega)\\ \|\nabla\varphi\|_{0,\Omega}=1}} (A\nabla(u - u_{Hh}), \nabla\varphi)_{\mathscr{P}}\,, \end{aligned} \tag{5.15}$$

where we used that (5.11) implies $(A\nabla(s - u_{Hh}), \nabla\varphi)_{\mathscr{P}} = 0$. Let now $\varphi \in H_0^1(\Omega)$ with $\|\varphi\|_{0,\Omega} = 1$ be fixed. Using the weak formulation (2.1), adding and subtracting $(\boldsymbol{\sigma}_h, \nabla\varphi)_{\mathscr{P}}$, $\boldsymbol{\sigma}_h \in H(\mathrm{div};\Omega)$ defined in (5.1) and integration by parts, we have

$$(A\nabla(u - u_{Hh}), \nabla\varphi)_{\mathscr{P}} = (f - \nabla\cdot\boldsymbol{\sigma}_h, \varphi)_{\mathscr{P}} - (A\nabla u_{Hh} + \boldsymbol{\sigma}_h, \nabla\varphi)_{\mathscr{P}}\,. \tag{5.16}$$

The Cauchy-Schwarz inequality gives

$$\begin{aligned} -(A\nabla u_{Hh} + \boldsymbol{\sigma}_h, \nabla\varphi)_{\mathscr{P}} &\leq \sum_{K\in\mathscr{P}} \|A\nabla u_{Hh} + \boldsymbol{\sigma}_h\|_{0,K}\|\nabla\varphi\|_{0,K} \\ &= \sum_{K\in\mathscr{P}} \eta_{1,K}\|\nabla\varphi\|_{0,K}\,, \end{aligned} \tag{5.17}$$

and from Proposition 4.2, the Poincaré inequality and Cauchy-Schwarz inequality,

$$\begin{aligned}(f-\nabla\cdot\boldsymbol{\sigma}_h,\varphi)_{\mathscr{P}} &= \sum_{K\in\mathscr{P}}(f-\Pi_{K,m}(\nabla\cdot\boldsymbol{\sigma}_h),\varphi)_K+(\Pi_{K,m}(\nabla\cdot\boldsymbol{\sigma}_h)-\nabla\cdot\boldsymbol{\sigma}_h,\varphi)_K\\ &= \sum_{K\in\mathscr{P}}(f-\Pi_{K,m}(f),\varphi-\overline{\varphi}_K)_K\\ &\quad+\sum_{K\in\mathscr{P}}(\Pi_{K,m}(\nabla\cdot\boldsymbol{\sigma}_h)-\nabla\cdot\boldsymbol{\sigma}_h,\varphi-\overline{\varphi}_K)_K\\ &\le \sum_{K\in\mathscr{P}}\frac{\mathcal{H}_K}{\pi}\|f-\Pi_{K,m}(f)\|_{0,K}\|\nabla\varphi\|_{0,K}\\ &\quad+\sum_{K\in\mathscr{P}}\frac{\mathcal{H}_K}{\pi}\|\Pi_{K,m}(\nabla\cdot\boldsymbol{\sigma}_h)-\nabla\cdot\boldsymbol{\sigma}_h\|_{0,K}\|\nabla\varphi\|_{0,K}\\ &= \sum_{K\in\mathscr{P}}\eta^f_{\mathrm{osc},K}\|\nabla\varphi\|_{0,K}+\sum_{K\in\mathscr{P}}\eta_{3,K}\|\nabla\varphi\|_{0,K} \qquad (5.18)\end{aligned}$$

where $\overline{\varphi}_K := (\varphi,1)/|K|$ and $\Pi_{K,m}(\cdot)$ is defined in (3.5). Combining (5.15)-(5.18),

$$\begin{aligned}\|A^{1/2}\nabla(u-s)\|^2_{0,\Omega} &\le \left(\sup_{\substack{\varphi\in H^1_0(\Omega)\\ \|\nabla\varphi\|_{0,\Omega}=1}}\sum_{K\in\mathscr{P}}(\eta_{1,K}+\eta^f_{\mathrm{osc},K}+\eta_{3,K})\|\nabla\varphi\|_{0,K}\right)^2\\ &\le \sum_{K\in\mathscr{P}}(\eta_{1,K}+\eta^f_{\mathrm{osc},K}+\eta_{3,K})^2\,, \qquad (5.19)\end{aligned}$$

and, then, from (5.14) and (5.19) we obtain the reliability estimate (5.6).

Now, for the lower bound, from [40, Theorem 4.2] and for every $F\in\mathcal{E}_H^K$ and $\mathfrak{f}\in\mathcal{F}_h^K\cap F$, it follows that

$$\begin{aligned}\eta_{2,K}=\|A^{1/2}\nabla(u_{Hh}-I_{OS}(u_{Hh}))\|_{0,K} &\le C\left\{\sum_{F\in\mathcal{E}_H^K}\sum_{\mathfrak{f}\in\mathcal{F}_h^K\cap F}h_{\mathfrak{f}}^{-1}\|[\![u_{Hh}]\!]\|^2_{0,\mathfrak{f}}\right\}^{1/2}\\ &\le C\left\{\sum_{F\in\mathcal{E}_H^K}\frac{H_F}{H_F\min_{\mathfrak{f}\subset F}h_{\mathfrak{f}}}\|[\![u_{Hh}]\!]\|^2_{0,F}\right\}^{1/2}.\end{aligned}$$

Let $F\in\mathcal{E}_H^K$. Using $\mu_H\in\Lambda_H$ given by $\mu_H=1$ in F and $\mu_H=0$ elsewhere, in the first equation of the MHM method (3.10) we get $\langle[\![u_{Hh}]\!],1\rangle_F=0$. So, applying [2, Theorem 10] we get

$$H_F^{-1}\|[\![u_{Hh}]\!]\|^2_{0,F}\le C\,\|A^{1/2}\nabla(u-u_{Hh})\|^2_{0,\tilde{\omega}_F}\le C\,\|A^{1/2}\nabla(u-u_{Hh})\|^2_{0,K\cup K'}\,,$$

where $\tilde{\omega}_F=\kappa_F\cup\tilde{\kappa}_F$, $\kappa_F\subseteq K$ and $\tilde{\kappa}_F\subseteq K'$ with $\kappa_F\in\Xi_H^K$ and $\tilde{\kappa}_F\in\Xi_H^{K'}$. For all $K\in\mathscr{P}$,

$$\sum_{F\in\mathcal{E}_H^K}\frac{H_F}{H_F\min_{\mathfrak{f}\subset F}h_{\mathfrak{f}}}\|[\![u_{Hh}]\!]\|^2_{0,F}\le C\sum_{F\in\mathcal{E}_H^K}\frac{H_F}{\min_{\mathfrak{f}\subset F}h_{\mathfrak{f}}}\|A^{1/2}\nabla(u-u_{Hh})\|^2_{0,\omega_K^F}\,.$$

Therefore,

$$\begin{aligned}\eta_{2,K}&=\|A^{1/2}\nabla(u_{Hh}-I_{OS}(u_{Hh}))\|_{0,K}\\ &\le C\left\{\sum_{F\in\mathcal{E}_H^K}\frac{H_F}{\min_{\mathfrak{f}\subset F}h_{\mathfrak{f}}}\|A^{1/2}\nabla(u-u_{Hh})\|^2_{0,\omega_K^F}\right\}^{1/2}.\end{aligned}$$

Let us now bound $\eta_{3,K}$. Recalling that $\nabla \cdot \boldsymbol{\sigma} = f$ in K, using the inverse inequality in $T \in \mathscr{T}_h^K$, (4.16), we get

$$
\begin{aligned}
\eta_{3,K} &\leq \frac{\mathcal{H}_K}{\pi}\|\Pi_{K,m}(\nabla \cdot \boldsymbol{\sigma}_h) - f\|_{0,K} + \frac{\mathcal{H}_K}{\pi}\|f - \nabla \cdot \boldsymbol{\sigma}_h\|_{0,K} \\
&\leq \eta^f_{\mathrm{osc},K} + \frac{\mathcal{H}_K}{\pi}\|f - \nabla \cdot \pi_K^{\mathcal{RT}_m}\boldsymbol{\sigma}\|_{0,K} + \frac{\mathcal{H}_K}{\pi}\|\nabla \cdot \pi_K^{\mathcal{RT}_m}\boldsymbol{\sigma} - \nabla \cdot \boldsymbol{\sigma}_h\|_{0,K} \\
&\leq C\,\eta^f_{\mathrm{osc},K} + C\left(\sum_{T\in\mathscr{T}_h^K}\frac{\mathcal{H}_K^2 h_T^2}{h_T^2}\|\nabla \cdot \pi_K^{\mathcal{RT}_m}\boldsymbol{\sigma} - \nabla \cdot \boldsymbol{\sigma}_h\|^2_{0,T}\right)^{1/2} \\
&\leq C\,\eta^f_{\mathrm{osc},K} + C\left(\sum_{T\in\mathscr{T}_h^K}\frac{\mathcal{H}_K^2}{h_T^2}\|\pi_T^{\mathcal{RT}_m}\boldsymbol{\sigma} - \boldsymbol{\sigma}_h\|^2_{0,T}\right)^{1/2} \\
&\quad + C\left(\sum_{T\in\mathscr{T}_h^K}\frac{\mathcal{H}_K^2}{h_T^2}\left\{\|A^{1/2}\nabla(u-u_{Hh})\|^2_{0,T} + h_T\|\Pi_{\mathcal{E},m}(\lambda) - \lambda_H\|^2_{0,\partial K}\right\}\right)^{1/2}.
\end{aligned}
$$

To bound $\eta_{1,K}$ we notice that, since $\boldsymbol{\sigma} = -A\nabla u \in H(\mathrm{div};\Omega)\cap H^s(\Omega)^d$, $s > 1/2$, then $\lambda \in L^2(\mathcal{E})$, so using the triangle inequality and (4.16) we get

$$
\begin{aligned}
\eta_{1,K} &= \|A\nabla\, u_{Hh} + \boldsymbol{\sigma}_h\|_{0,K} \\
&\leq \|A\nabla u_{Hh} + \boldsymbol{\sigma}\|_{0,K} + \|\boldsymbol{\sigma} - \pi_K^{\mathcal{RT}_m}\boldsymbol{\sigma}\|_{0,K} + \|\pi_K^{\mathcal{RT}_m}\boldsymbol{\sigma} - \boldsymbol{\sigma}_h\|_{0,K} \\
&\leq C\,\|A\nabla(u-u_{Hh})\|_{0,K} + \eta^{\boldsymbol{\sigma}}_{\mathrm{ho},K} + \mathcal{H}_K^{1/2}\|\Pi_{\mathcal{E},m}(\lambda) - \lambda_H\|_{0,\partial K}\,.
\end{aligned}
$$

Finally, using the assumption about the mesh parameters and adding in $K \in \mathscr{P}$, we get (5.10) which finishes the proof. □

Remark 5.3 (The one-element submesh case)**.** *When $\mathscr{P}$ is a simplicial triangulation and $\mathscr{T}_h^K = \{K\}$, and $h = H = \mathcal{H}$, then $\Pi_{K,m}(\nabla \cdot \boldsymbol{\sigma}_h) = \nabla \cdot \boldsymbol{\sigma}_h$ for all $K \in \mathscr{P}$ and $\ell \leq m \leq k$, which implies that $\eta_{3,K}$ disappears from the aposterior estimator in* (5.6)*. Also, the dependence of the lower bound for $\eta_{2,K}$ on the ratio H/h in* (5.8) *does no appear.*

Assumption C and the factor $\mathcal{H}/h$ in the efficiency estimates for $\eta_{3,K}$ in (5.8) appear as the price to pay for deriving a fully computable *a posteriori* error estimator. Next remarks present an alternative estimator that does not require Assumption C and has "cleaner" lower bounds, but is not fully computable. It is important to note that the factor H/h in the lower bound for $\eta_{2,K}$ in (5.8) is always present in multilevel discretizations, but differs from the factor $\mathcal{H}/h$ in [40] involving the coarser scale $\mathcal{H}$.

Remark 5.4 (Relaxing Assumption C)**.** *Assumption C allows us to have a fully computable a posteriori error bound. However, if we do not take into account this assumption, we can still have an a posteriori error bound, only not fully computable. In the case where Assumption C is not satisfied, i.e., $K \in \mathscr{P}$ is not convex,* (5.7) *can be replaced by*

$$
\eta^f_{osc,K} := C_P\,\mathcal{H}_K\|f - \Pi_{K,m}(f)\|_{0,K}\,, \tag{5.20}
$$

and $C_P > 0$ is a constant independent of K according to the Poincaré-Wirtinger inequality, whose proof can be found in [43, Theorem 3.2].

Remark 5.5 (Avoiding factor $\mathcal{H}/h$ in (5.8))**.** *The factor $\mathcal{H}/h$ in the efficiency estimates for $\eta_{3,K}$ states that, for a fully computable upper bound, we may not use the approach where we fix $\mathcal{H}$ and make $H, h \to 0$. If we accept not having a fully computable upper bound, we recover the above said approach by replacing*

(5.5) *by*
(5.21)

$$\eta_{3,K} := \left\{ \sum_{T\in\mathscr{T}_h^K} \eta_{3,T}^2 \right\}^{1/2} = \left\{ \sum_{T\in\mathscr{T}_h^K} h_T^2 \, \|\Pi_{T,m}(\nabla\cdot\boldsymbol{\sigma}_h) - \nabla\cdot\boldsymbol{\sigma}_h\|_{0,T}^2 \right\}^{1/2} .$$

In fact, the estimate (5.6) *can be rewritten as (see Appendix A for details)*

$$\|A^{1/2}\nabla(u-u_{Hh})\|_{0,\mathscr{P}}^2 \leq C\,\eta^2 \leq C \sum_{K\in\mathscr{P}} (\eta_{1,K}+\eta_{osc,K}^f+\eta_{3,K})^2 + \sum_{K\in\mathscr{P}} \eta_{2,K}^2 , \tag{5.22}$$

with an unknown constant C*, where we used* (5.20) *and* (5.21) *instead of* (5.7) *and* (5.5)*. Following analogous steps used in Theorem 5.1, the lower bound for the alternative* $\eta_{3,K}$ *in* (5.21) *reads*
(5.23)

$$\eta_{3,K} \leq C \left(\|A^{1/2}\nabla(u-u_{Hh})\|_{0,K} + \mathcal{H}_K^{1/2} \|\Pi_{\mathcal{E},m}(\lambda) - \lambda_H\|_{0,\partial K} + \eta_{osc,K}^f \right) ,$$

which no longer depends on the factor $\mathcal{H}/h$*.*

6. Numerical Results

This section verifies the theoretical aspects of this work. The following numerical results are based on an implementation using FreeFem++ [32]. Since one of the objectives is to validate the *a posteriori* error estimates, we build $\boldsymbol{\sigma}_h$ using $\ell \leq m \leq k$ with $k \geq \ell + d$ defined in (5.1) on conforming meshes. The expected orders of convergence are given by Table 1.

Error estimates	**Order**
$\|u - u_{Hh}\|_{1,\Omega}$	$h^k + H^{\ell+1}$
$\|\boldsymbol{\sigma} - \boldsymbol{\sigma}_h\|_{0,\Omega}$	$h^k + H^{\ell+1}$
$\|\nabla\cdot\boldsymbol{\sigma} - \nabla\cdot\boldsymbol{\sigma}_h\|_{0,\Omega}$	$h^{k-1} + H^{\ell}$
$\|\nabla\cdot\boldsymbol{\sigma} - \Pi_{\Omega,m}(\nabla\cdot\boldsymbol{\sigma}_h)\|_{0,\Omega}$	h^{m+1}

Table 1. Error estimates order for $\ell \geq 0$, $k \geq \ell + d$ and $\ell \leq m \leq k$.

6.1. **A smooth case with an analytical solution.** The goal of this experiment is to assess the theoretical results using a smooth analytical solution. We consider $A = Id$, and the right-hand side and boundary conditions are chosen such that

$$u(x,y) = \sin(2\pi x)\sin(2\pi y) ,$$

solves (2.1). Here we are using a conforming mesh where both global and local meshes are based on triangles.

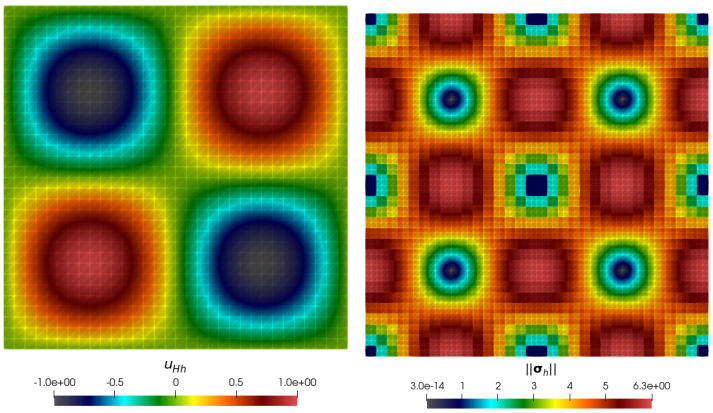

Figure 2. The solution u_{Hh} (left) and the magnitude of $\boldsymbol{\sigma}_h$ from the flux recovery strategy (right).

Figure 2 shows the approximate solution, u_{Hh}, computed through the MHM method (3.10) using $\ell = 0$ and $k = 2$ and the magnitude of the approximate flux $\boldsymbol{\sigma}_h$ built using the flux recovery strategy in (5.1) for $m = 2$.

The convergence results in the $L^2(\Omega)-$norm for the flux variable $\boldsymbol{\sigma}_h$ using the solution of the MHM method with $\ell \in \{0, 1\}$ and $k \in \{2, 3\}$ in a conforming mesh are depicted in Figure 3.

We observe a convergence which is consistent with the theoretical error estimates. In fact, the theoretical results predict that the $L^2(\Omega)-$norm for the flux, as derived from the recovery strategy, exhibit a convergence rate of $\mathcal{O}(H^{\ell+1})$. Furthermore, according to Remark 5.1, we can also see in Figure 3 that using $\ell \leq m \leq k$ for a conforming mesh, the projection of the divergence of $\boldsymbol{\sigma}_h$ converges at rate $\mathcal{O}(h^{m+1})$.

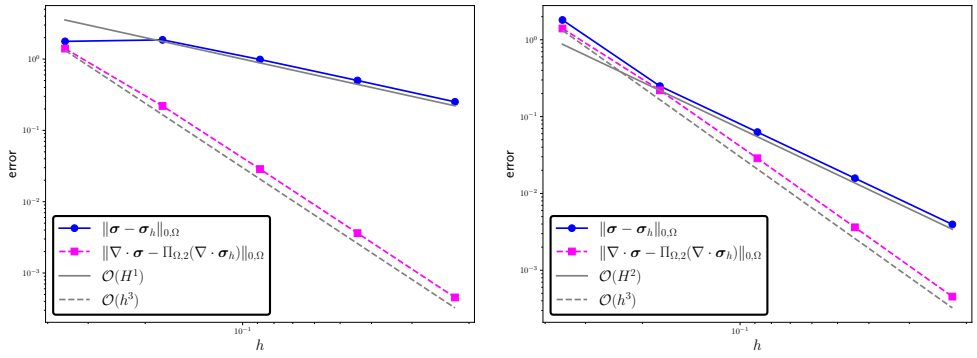

FIGURE 3. The convergence on simplicial elements in the $L^2(\Omega)-$norm for $\ell = 0$ (left) and $\ell = 1$(right) and $\boldsymbol{\sigma}_h$ with $m = 2$. Here $h = \frac{\mathcal{H}}{2}$ and $k = \ell + 2$.

Figure 4 shows a comparison between the divergence of the flux obtained through simple post-processing of the primal variable, namely $-A\nabla u_{Hh}$, and the flux obtained from (5.1), with $\ell = 0$, $k = 2$ and $m = 2$. It is interesting to note that $\boldsymbol{\sigma}_h$ from our proposed strategy converges with the optimal order of $\mathcal{O}(h^{m+1})$ in the $L^2(\Omega)-$norm while the other approach does not converge in the broken semi-norm

$$\|\nabla\cdot\boldsymbol{\tau}\|^2_{0,\mathscr{T}_h} := \sum_{K\in\mathscr{P}}\sum_{T\in\mathscr{T}_h^K}\|\nabla\cdot\boldsymbol{\tau}\|^2_{0,T} \qquad \forall\boldsymbol{\tau}\in H(\mathrm{div};\mathscr{T}_h)\,.$$

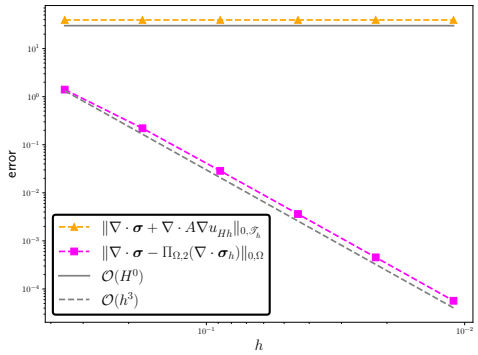

FIGURE 4. The convergence on simplicial elements for the $L^2(\Omega)-$norm for the divergence with $\ell = 0$, $k = 2$ and $m = 2$. Here $h = \frac{\mathcal{H}}{2}$.

The convergence results in the $H(\mathrm{div};\Omega)$-norm for the recovered flux variable $\boldsymbol{\sigma}_h$, obtained using the MHM method with $\ell \in \{1, 2\}$, $k = 3$, and $m = 2$ on a conforming mesh, are shown in Figure 5. The results confirm the convergence rate of order $\mathcal{O}(H^\ell)$, as predicted by the theory.

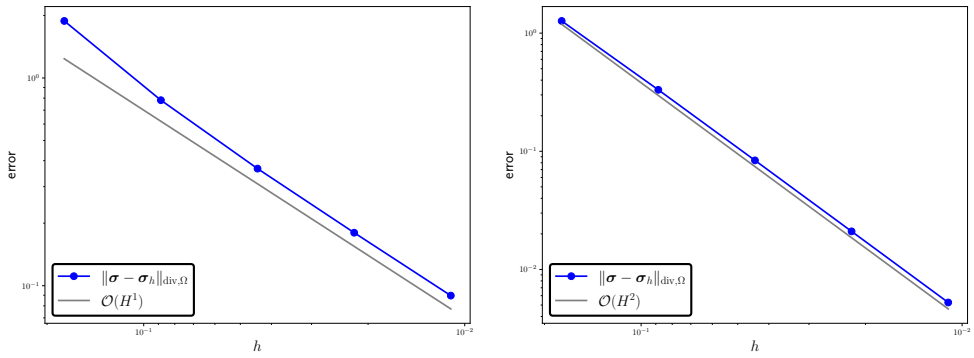

FIGURE 5. The convergence on simplicial elements for the $H(\mathrm{div};\Omega)-$norm for the recovered flux with $\ell = 1$ (left) and $\ell = 2$ (right). Here $k = 3$, $m = 2$ and $h = \frac{\mathcal{H}}{2}$.

Now, regarding the *a posteriori* estimator defined in Section 5, Tables 2 and 3 report the error in the energy norm $\|A^{1/2}\nabla(u-u_{Hh})\|_{0,\mathscr{P}}$, the global estimator η given in Theorem 5.1 as well as the individual estimators $\eta_1 := \|A\nabla u_{Hh} + \boldsymbol{\sigma}_h\|_{0,\mathscr{P}}$, $\eta_2 := \|A^{1/2}\nabla(u_{Hh}-I_{OS}(u_{Hh}))\|_{0,\mathscr{P}}$, $\eta_3 := \frac{\mathcal{H}}{\pi}\|\Pi_{\Omega,m}(\nabla\cdot\boldsymbol{\sigma}_h)-\nabla\cdot\boldsymbol{\sigma}_h\|_{0,\mathscr{P}}$, and the oscillation and high-order terms η^f_{osc} and $\eta^{\boldsymbol{\sigma}}_{ho}$ for the MHM solution with $\ell = \{0,1\}$, $k = \{2,3\}$, and for the flux recovery strategy with $m = 2$. We can observe that η^f_{osc} and $\eta^{\boldsymbol{\sigma}}_{ho}$ are indeed oscillation and high-order terms and the estimator get tighter.

Tables 2 and 3 also reports the effectivity indices (overestimation factor) defined as

$$I^{eff} := \frac{\eta}{\|A^{1/2}\nabla(u-u_{Hh})\|_{0,\mathscr{P}}},$$

and the corresponding orders of convergence in parentheses. As predicted by theory, the estimator η is a strict upper bound on the discretization error. The effectiveness indices (see Tables 2 and 3) also show robust behavior.

$\mathcal{H}$	ℓ	k	m	$\|A^{1/2}\nabla(u-u_{Hh})\|_{0,\mathscr{P}}$	η_1	η_2	η_3	η^f_{osc}	$\eta^{\boldsymbol{\sigma}}_{ho}$	η	I^{eff}
0.353	0	2	2	1.860	0.149	2.447	1.186	0.016	0.008	2.724	1.463
0.176				0.986 (0.91)	0.031 (2.25)	1.265 (0.95)	0.266 (2.15)	0.001 (3.91)	0.001 (3.06)	1.293 (1.07)	1.311
0.088				0.501 (0.97)	0.007 (2.09)	0.641 (0.97)	0.064 (2.00)	6.77e-05 (3.97)	1.23e-04 (3.01)	0.644 (1.00)	1.287
0.044				0.251 (0.99)	0.001 (2.02)	0.323 (0.99)	0.015 (2.01)	4.24e-06 (3.99)	1.54e-05 (3.00)	0.323 (0.99)	1.285
0.022				0.125 (0.99)	4.45e-04 (2.00)	0.162 (0.99)	0.003 (2.00)	2.65e-07 (3.99)	1.92e-06 (3.00)	0.162 (0.99)	1.287

TABLE 2. Numerical validation of the a posteriori error estimator η with $\ell = 0$ and $k = 2$. Here $h = \frac{\mathcal{H}}{2}$.

$\mathcal{H}$	ℓ	k	m	$\|A^{1/2}\nabla(u-u_{Hh})\|_{0,\mathscr{P}}$	η_1	η_2	η_3	η^f_{osc}	$\eta^{\boldsymbol{\sigma}}_{ho}$	η	I^{eff}
0.353	1	3	2	0.242	0.048	0.292	0.430	0.016	0.008	0.522	2.152
0.176				0.060 (1.99)	0.012 (1.98)	0.074 (1.97)	0.094 (2.19)	0.001 (3.91)	0.001 (3.06)	0.120 (2.11)	1.977
0.088				0.015 (1.99)	0.003 (1.99)	0.018 (1.98)	0.022 (2.06)	6.77e-05 (3.97)	1.23e-04 (3.01)	0.029 (2.03)	1.923
0.044				0.003 (1.99)	7.74e-04 (2.00)	0.004 (1.99)	0.005 (2.02)	4.24e-06 (3.99)	1.54e-05 (3.00)	0.007 (2.00)	1.907
0.022				9.57e-04 (1.99)	1.93e-04 (2.00)	0.001 (1.99)	0.001 (2.00)	2.65e-07 (3.99)	1.92e-06 (3.00)	0.001 (2.00)	1.902

TABLE 3. Numerical validation of the a posteriori error estimator η with $\ell = 1$ and $k = 3$. Here $h = \frac{\mathcal{H}}{2}$.

In the particular case where $h = H = \mathcal{H}$, we obtain that η_3 in (5.5) vanishes, since $\mathscr{T}_h^K = \{K\}$, and efining the mesh, we find that the effectiveness indices tends to approximately 1.09 for $\ell = 0$ and 1.52 for $\ell = 1$. By refining only the submesh (from $h = \mathcal{H}/2$ to $h = \mathcal{H}/8$) and keeping H fixed, we observe an increase in the effectiveness indices (from 1.52 to 2.42 for $\ell = 1$, for example) as predicted by the local lower bound in Theorem 5.1. The results show that the estimates of Theorem 5.1 are accurate and the estimator shows competitive performance, consistent with observations reported in the literature [34, 40, 27], despite the influence of the submesh on the effectiveness indices. To the best of our knowledge, avoiding estimator dependence on subgrids remains an open question in the literature.

6.2. **SPE 10.** We use Model 2 of the 10th Society of Petroleum Engineers Comparative Solution Project (c.f. [16]) hereafter referred to as the SPE-10 model.

To validate our flux recovery strategy described in (5.1), we choose layer 36 as the object of our study and set the entry pressures as $u = 1$ (bottom) and exit $u = 0$ (top). On the other two boundaries, we set homogeneous Neumann conditions.

Since this benchmark does not have an analytical solution, we used a standard mixed formulation using Raviart-Thomas spaces of order 2 on a mesh of 125.000 triangular elements and 1.314.000 degrees of freedom to obtain a reference solution for this case.

Figure 6 shows that the magnitude of the discrete flux $\boldsymbol{\sigma}_h$, from the flux recovery strategy in (5.1) with $m = 2$, approximates the canal better than the current approximation done in the MHM method using $-A\nabla u_{Hh}$.

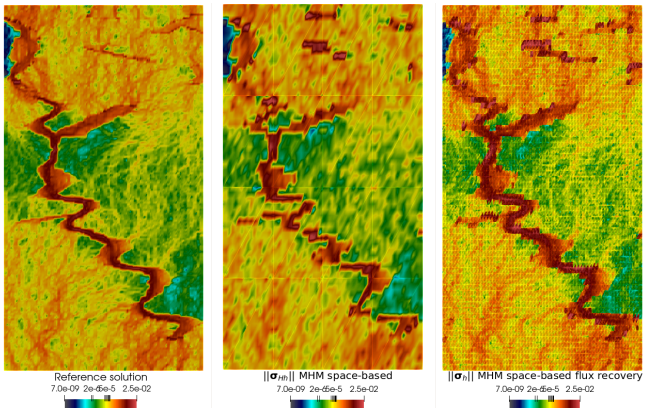

FIGURE 6. The reference solution (left). The dual variable obtained from $-A\nabla u_{Hh}$ (middle) and from the flux recovery strategy with $m = 2$ (right) using the MHM method with $\ell = 0$ and $k = 2$.

We next test the performance of the *a posteriori* estimator defined in (5.6). We start with a coarse initial mesh of 512 elements and 4 elements in the submesh and build an adaptive algorithm based on the remeshing routine in FreeFem++ (see [32, Section 5.1.9] for a complete description). In Figure 7 we depict a sequence of adapted meshes obtained with this strategy while in Figure 8, the magnitude of $\boldsymbol{\sigma}_h$ is depicted in the first and last meshes along with the reference solution. The last adapted mesh has 3.786 elements and 9.559 degrees of freedom.

Finally, in Figure 9 we depict a diagonal cross-section of u_{Hh} from $(0, 0)$ to $(1200, 2200)$ where we can observe the improvement induced by the use of adaptive meshes.

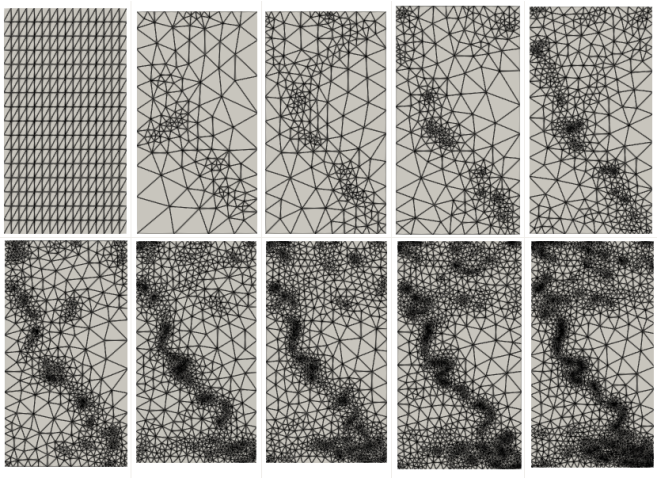

FIGURE 7. Sequence of adapted meshes induced by the *a posteriori* estimator η. Here $\ell = 0$.

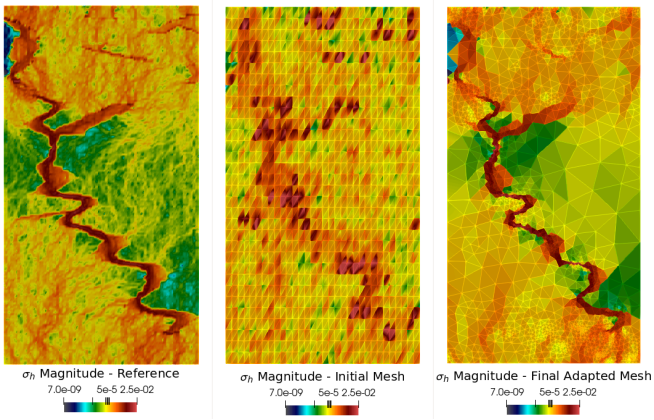

FIGURE 8. Isolines of $|\boldsymbol{\sigma}_h|$ obtained from the reference solution (left) and from the MHM method using the initial mesh (middle) and the adapted mesh (right).

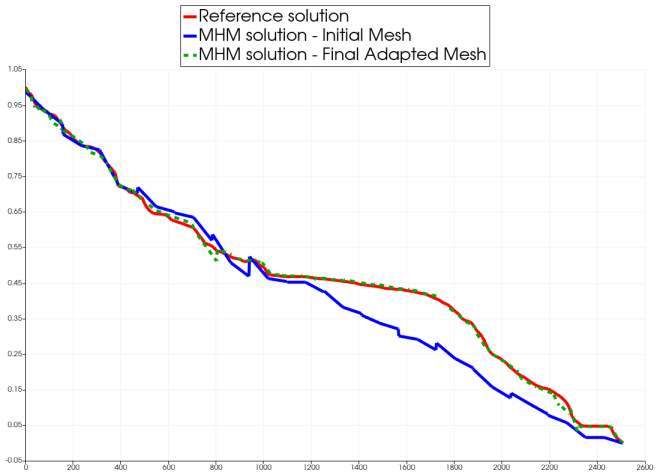

FIGURE 9. Comparison of the profile of the reference solution and the MHM's solution u_{Hh} obtained on the initial and final adapt meshes. Here $\ell = 0$.

7. CONCLUSIONS

In this work, we have introduced a localized post-processing strategy designed to construct an approximate flux based on the solution derived from

the MHM method. Also, as a by-product of the flux recovery strategy, we introduced and analyzed an *a posteriori* error estimator.

The main contribution is regarding how we deal with the flux recovery when we take into account face mesh partitions and second-level meshes in the MHM method. This is exactly the scenario when the MHM method is used to approximate the solution of multiscale problems. We proposed a new cheap, local system to post-process the dual variable and, following this, we conducted a convergence analysis. We proved that this approximation achieves optimal convergence orders of $\mathcal{O}(H^{\ell+1})$ in the $L^2(\Omega)-$norm for $\boldsymbol{\sigma}_h$. Additionally, we proved that refining only the second-level mesh leads to optimal convergence order of $\mathcal{O}(h^{\ell+1})$ ($\mathcal{O}(h^{m+1})$, $\ell \leq m \leq k$ and $k \geq \ell + d$, when considering a conforming mesh) for the $L^2(\Omega)-$norm of $\Pi_{\Omega,m}(\nabla \cdot \boldsymbol{\sigma}_h)$, which contrasts to the conventional approach of using $-A\nabla u_{Hh}$ in the MHM method, for which optimal convergence does not occur.

Finally, we have proposed a fully computable *a posteriori* error estimator using both the approximate solution u_{Hh} and the approximate flux $\boldsymbol{\sigma}_h$ derived from the flux recovery strategy. The *a posteriori* error estimate provides a strict, fully computable, upper bound for the error $u-u_{Hh}$. Also, under appropriate regularity assumptions (linked to natural assumptions for the analysis of the MHM method) it provides a lower bound for an enhanced norm of the error. The possibility of removing the extra term from a posteriori estimates of MHM methods remains an open problem.

Appendix A. Technical results

Let $b_{\mathfrak{f}}$ be the bubble function with support in $\omega_{\mathfrak{f}} \in \mathcal{F}_h^K$ defined with respect to the barycentric coordinates (see for instance [3, Section 2.3.1] for details. For the sake of completeness, we line up the following theorem that summarizes the main properties of these functions.

Theorem A.1. *Let $\mathfrak{f} \in \mathcal{F}_h^K$ be a facet and let $b_{\mathfrak{f}}$ be the corresponding bubble function. Then there exists a positive constant C such that for all $v \in \mathbb{P}_t(T), t \geq 0$, the following holds*

$$C^{-1}\|v\|_{0,\mathfrak{f}}^2 \leq (b_{\mathfrak{f}}\, v, v)_{\mathfrak{f}} \leq C\|v\|_{0,\mathfrak{f}}^2\,, \tag{A.1}$$

and

$$h_T^{-1/2}\|b_{\mathfrak{f}}\, v\|_{0,T} + h_T^{1/2}|b_{\mathfrak{f}}\, v|_{1,T} \leq C\|v\|_{0,\mathfrak{f}}\,, \tag{A.2}$$

where the constant C is independent of v and h_T.

We will define some notations in each subelement $T \in \mathscr{T}_h^K$ and on each subface $\mathfrak{f} \in \mathcal{F}_h^K \cap \partial T$, particularly, regarding internal faces. They are the following:

$$R_T := (f + \nabla \cdot A\nabla u_{Hh})|_T \quad \forall\, T \in \mathscr{T}_h^K\,, \tag{A.3}$$

and on $\mathfrak{f} \in \mathcal{F}_0^K \cap \partial T$,

$$R_{\mathfrak{f}} := \left(A\nabla u_{Hh}|_T + \pi_T^{\mathcal{RT}_\ell}\boldsymbol{\sigma}\right) \cdot \boldsymbol{n}_{\mathfrak{f}}\,. \tag{A.4}$$

Theorem A.2. *Let $K \in \mathscr{P}$. For $T \in \mathscr{T}_h^K$ the following holds*

$$\|R_T\|_{0,T} \leq C\, h_T^{-1}|u - u_{Hh}|_{1,T}\,. \tag{A.5}$$

Furthermore, for $\mathfrak{f} \in \mathcal{F}_0^K \cap \partial T$ we have that

$$\|R_{\mathfrak{f}}\|_{0,\mathfrak{f}} \leq C\, \left(h_T^{1/2}\|R_T\|_{0,T} + h_T^{-1/2}|u - u_{Hh}|_{1,T} + \|\pi_T^{\mathcal{RT}_\ell}\boldsymbol{\sigma} - \boldsymbol{\sigma}\|_{0,\partial T}\right)\,, \tag{A.6}$$

where C is a positive constant independent of H and h.

Proof. Let $K \in \mathscr{P}$, $T \in \mathscr{T}_h^K$ and $\mathfrak{f} \in \mathcal{F}_h^K \cap \partial T$. We define $\beta_\mathfrak{f} := b_\mathfrak{f} P_\mathfrak{f}(R_\mathfrak{f})$, where $P_\mathfrak{f} : \mathbb{P}_k(\mathfrak{f}) \to \mathbb{P}_k(\omega_\mathfrak{f})$ is an extension of functions defined on a face $\mathfrak{f}$ to the patch $\omega_\mathfrak{f} = T \cup T'$. The proof of (A.5) follows identical steps to those from [5, Theorem 4.3]

Let $\mathfrak{f} \in \mathcal{F}_0^K \cap \partial T$, then

$$(R_\mathfrak{f}, \beta_\mathfrak{f})_\mathfrak{f} = ((A\nabla u_{Hh}|_T + \pi_T^{\mathcal{RT}_\ell}\boldsymbol{\sigma}) \cdot \boldsymbol{n}_\mathfrak{f}, \beta_\mathfrak{f})_\mathfrak{f}\,.$$

Using that $\beta_\mathfrak{f}|_{\partial T \setminus \mathfrak{f}} = 0$, integration by parts, (A.3), we get

$$\begin{aligned}
((A\nabla u_{Hh}|_T + \pi_T^{\mathcal{RT}_\ell}\boldsymbol{\sigma}) \cdot \boldsymbol{n}_\mathfrak{f}, \beta_\mathfrak{f})_\mathfrak{f} &= (\nabla \cdot A\nabla u_{Hh}, \beta_\mathfrak{f})_T + (A\nabla u_{Hh}, \nabla\beta_\mathfrak{f})_T \\
&\quad + (\pi_T^{\mathcal{RT}_\ell}\boldsymbol{\sigma} \cdot \boldsymbol{n}_\mathfrak{f}, \beta_\mathfrak{f})_{\partial T} \\
&= (\nabla \cdot A\nabla u_{Hh} + f, \beta_\mathfrak{f})_T + (A\nabla u_{Hh}, \nabla\beta_\mathfrak{f})_T \\
&\quad + (\nabla \cdot A\nabla u, \beta_\mathfrak{f})_T + (\pi_T^{\mathcal{RT}_\ell}\boldsymbol{\sigma} \cdot \boldsymbol{n}_\mathfrak{f}, \beta_\mathfrak{f})_{\partial T} \\
&= (R_T, \beta_\mathfrak{f})_T + (A\nabla(u_{Hh} - u), \nabla\beta_\mathfrak{f})_T \\
&\quad + ((A\nabla u + \pi_T^{\mathcal{RT}_\ell}\boldsymbol{\sigma}) \cdot \boldsymbol{n}_\mathfrak{f}, \beta_\mathfrak{f})_{\partial T} \\
&= (R_T, \beta_\mathfrak{f})_T + (A\nabla(u_{Hh} - u), \nabla\beta_\mathfrak{f})_T \\
&\quad + ((\pi_T^{\mathcal{RT}_\ell}\boldsymbol{\sigma} - \boldsymbol{\sigma}) \cdot \boldsymbol{n}_\mathfrak{f}, \beta_\mathfrak{f} - \bar{\beta}_\mathfrak{f})_{\partial T}\,,
\end{aligned}$$

where $\bar{\beta}_\mathfrak{f}$ denotes the mean value of $\beta_\mathfrak{f}$ on T, and in the last equation we used the interpolation property of the operator $\pi_T^{\mathcal{RT}_\ell}$. Therefore, using the stability of the operator $P_\mathfrak{f}$, the definition of $\beta_\mathfrak{f}$, Cauchy-Schwarz inequality, trace inequality (see [22, Remark 12.17]) and (A.2), we get

$$\begin{aligned}
\|R_\mathfrak{f}\|_{0,\mathfrak{f}}^2 &\le C\left(\|R_T\|_{0,T}\|\beta_\mathfrak{f}\|_{0,T} + |u - u_{Hh}|_{1,T}|\beta_\mathfrak{f}|_{1,T} + h_T^{1/2}\|\pi_T^{\mathcal{RT}_\ell}\boldsymbol{\sigma} - \boldsymbol{\sigma}\|_{0,\partial T}|\beta_\mathfrak{f}|_{1,T}\right) \\
&\le C\left(\|R_T\|_{0,T}h_T^{1/2}\|R_\mathfrak{f}\|_{0,\mathfrak{f}} + |u - u_{Hh}|_{1,T}h_T^{-1/2}\|R_\mathfrak{f}\|_{0,\mathfrak{f}}\right. \\
&\quad \left. + \|\pi_T^{\mathcal{RT}_\ell}\boldsymbol{\sigma} - \boldsymbol{\sigma}\|_{0,\partial T}\|R_\mathfrak{f}\|_{0,\mathfrak{f}}\right) \\
&= C\left(h_T^{1/2}\|R_T\|_{0,T} + h_T^{-1/2}|u - u_{Hh}|_{1,T} + \|\pi_T^{\mathcal{RT}_\ell}\boldsymbol{\sigma} - \boldsymbol{\sigma}\|_{0,\partial T}\right)\|R_\mathfrak{f}\|_{0,\mathfrak{f}}\,,
\end{aligned}$$

which finishes the proof.

□

We detail below the proof of (5.23), using the fact that the proof of estimate (5.18) may be revisited in a different way. More precisely, we now present the proof of (5.22).

Proof.

$$\begin{aligned}
(f - \nabla \cdot \boldsymbol{\sigma}_h, \varphi)_\mathscr{P} &= \sum_{K \in \mathscr{P}} (f - \Pi_{K,m}(\nabla \cdot \boldsymbol{\sigma}_h), \varphi)_K + (\Pi_{K,m}(\nabla \cdot \boldsymbol{\sigma}_h) - \nabla \cdot \boldsymbol{\sigma}_h, \varphi)_K \\
&= (a) + (b)\,.
\end{aligned}$$

For (a), we will consider (5.20), and then it holds

$$\begin{aligned}
(a) &= \sum_{K\in\mathscr{P}} (f - \Pi_{K,m}(f), \varphi)_K \\
&= \sum_{K\in\mathscr{P}} \sum_{T\in\mathscr{T}_h^K} (f - \Pi_{T,m}(f), \varphi - \Pi_{T,m}(\varphi))_T \\
&\leq \sum_{K\in\mathscr{P}} \sum_{T\in\mathscr{T}_h^K} \|f - \Pi_{T,m}(f)\|_{0,T} \|\varphi - \Pi_{T,m}(\varphi)\|_{0,T} \\
&\leq C \sum_{K\in\mathscr{P}} \left\{ \sum_{T\in\mathscr{T}_h^K} h_T^2 \|f - \Pi_{T,m}(f)\|_{0,T}^2 \right\}^{1/2} \|\nabla\varphi\|_{0,K} \\
&\leq C \sum_{K\in\mathscr{P}} \eta^f_{\mathrm{osc},K} \|\nabla\varphi\|_{0,K} \,.
\end{aligned}$$

Following analogous steps, for (b) we have,

$$\begin{aligned}
(b) &= \sum_{K\in\mathscr{P}} (\Pi_{K,m}(\nabla\cdot\boldsymbol{\sigma}_h) - \nabla\cdot\boldsymbol{\sigma}_h, \varphi)_K \\
&= \sum_{K\in\mathscr{P}} \sum_{T\in\mathscr{T}_h^K} (\Pi_{T,m}(\nabla\cdot\boldsymbol{\sigma}_h) - \nabla\cdot\boldsymbol{\sigma}_h, \varphi - \Pi_{T,m}(\varphi))_T \\
&\leq C \sum_{K\in\mathscr{P}} \sum_{T\in\mathscr{T}_h^K} \|\Pi_{T,m}(\nabla\cdot\boldsymbol{\sigma}_h) - \nabla\cdot\boldsymbol{\sigma}_h\|_{0,T} \|\varphi - \Pi_{T,m}(\varphi)\|_{0,T} \\
&\leq C \sum_{K\in\mathscr{P}} \left\{ \sum_{T\in\mathscr{T}_h^K} \eta_{3,T}^2 \right\}^{1/2} \|\nabla\varphi\|_{0,K} \,,
\end{aligned}$$

and the result follows. □

Acknowledgments

We would like to acknowledge the IPES research group (http://ipes.lncc.br/) for the valuable discussions and CNPq/Brazil and The London Mathematical Society for funding this research.

Funding

We would like to acknowledge the IPES research group (http://ipes.lncc.br/) for the valuable discussions and CNPq/Brazil and The London Mathematical Society for funding this research. This work was authored in part by the National Renewable Energy Laboratory, operated by Alliance for Sustainable Energy, LLC, for the U.S. Department of Energy (DOE) under Contract No. DE-AC36-08GO28308. The views expressed in the presentation do not necessarily represent the views of the DOE or the U.S. Government. The U.S. Government retains and the publisher, by accepting the article for publication, acknowledges that the U.S. Government retains a nonexclusive, paid-up, irrevocable, worldwide license to publish or reproduce the published form of this work, or allow others to do so, for U.S. Government purposes.

References

[1] A. Abdulle, W. E, B. Engquist, and E. Vanden-Eijnden. The heterogeneous multiscale methods. *Communications in Mathematical Sciences*, 1 (1):87–132, 2003.

[2] Y. Achdou, C. Bernardi, and F. Coquel. A priori and a posteriori analysis of finite volume discretizations of Darcy's equations. *Numerische Mathematik*, 96:17–42, 2003.

[3] M. Ainsworth and J.T. Oden. A posteriori error estimation in finite element analysis. *Computer Methods in Applied Mechanics and Engineering*, 142(1):1–88, 1997. ISSN 0045-7825.

[4] R. Araya, C. Harder, D. Paredes, and F. Valentin. Multiscale hybrid-mixed method. *SIAM Journal on Numerical Analysis*, 51(6):3505–3531, 2013.

[5] R. Araya, R. Rebolledo, and F. Valentin. On a multiscale a posteriori error estimator for the Stokes and Brinkman equations. *IMA Journal of Numerical Analysis*, 41(1):344–380, 2021.

[6] T. Arbogast, G. Pencheva, M. F. Wheeler, and I. Yotov. A multiscale mortar mixed finite element method. *SIAM Multiscale Modeling and Simulation*, 6:319–346, 2007.

[7] I. Babuska and E. Osborn. Generalized finite element methods: Their performance and their relation to mixed methods. *SIAM J. Num. Anal.*, 20(3):510–536, 1983.

[8] G. R. Barrenechea, L. P. Franca, and F. Valentin. A Petrov–Galerkin enriched method: A mass conservative finite element method for the Darcy equation. *Computer Methods in Applied Mechanics and Engineering*, 196 (21-24):2449–2464, 2007.

[9] G. R. Barrenechea, F. Jaillet, D. Paredes, and F. Valentin. The multiscale hybrid mixed method in general polygonal meshes. *Numerische Mathematik*, 145(1):197–237, 2020.

[10] G.A. Batistela, D. Siqueira, P.R.B. Devloo, and S.M. Gomes. A posteriori error estimator for a multiscale hybrid mixed method for darcy's flows. *International Journal for Numerical Methods in Enginnering*, 123(24): 6052–6078, 2022.

[11] D. Braess, V. Pillwein, and J. Schöberl. Equilibrated residual error estimates are p-robust. *Computer Methods in Applied Mechanics and Engineering*, 198(13-14):1189–1197, 2009.

[12] Z. Cai and S. Zhang. Flux recovery and a posteriori error estimators: conforming elements for scalar elliptic equations. *SIAM journal on numerical analysis*, 48(2):578–602, 2010.

[13] L. Chamoin and F. Legoll. A posteriori error estimation and adaptive strategy for the control of msfem computations. *Computer Methods in Applied Mechanics and Engineering*, 336:1–38, 2018.

[14] T. Chaumont-Frelet and M. Vohralík. Constrained and unconstrained stable discrete minimizations for p-robust local reconstructions in vertex patches in the de rham complex. *Foundations of Computational Mathematics*, pages 1–42, 2024.

[15] S.H. Chou, D. Kwak, and K. Kim. Flux recovery from primal hybrid finite element methods. *SIAM Journal on Numerical Analysis*, 40(2):403–415, 2002.

[16] M. A. Christie and M. J. Blunt. Tenth SPE comparative solution project: A comparison of upscaling techniques. In *SPE Reservoir Simulation Symposium*. Society of Petroleum Engineers, 2001.

[17] M. R. Correa and G. Taraschi. Optimal H(div) flux approximations from the primal hybrid finite element method on quadrilateral meshes. *Computer Methods in Applied Mechanics and Engineering*, 400:115539, 2022. ISSN 0045-7825.

[18] P. Destuynder and B. Métivet. Explicit error bounds in a conforming finite element method. *Mathematics of Computation*, 68(228):1379–1396, 1999.

[19] Ricardo G. Durán. *Mixed finite element methods*, pages 1–44. Springer Berlin Heidelberg, Berlin, Heidelberg, 2008.

[20] O. Durán, P. R.B. Devloo, S. M. Gomes, and F. Valentin. A multiscale hybrid method for Darcy's problems using mixed finite element local solvers. *Computer Methods in Applied Mechanics and Engineering*, 354:213–244, 2019. ISSN 0045-7825.

[21] Y. Efendiev, T.Y. Hou, and X.H. Wu. Convergence of a nonconforming multiscale finite element method. *SIAM J. Numer. Anal.*, 37(3):888–910, 2000.

[22] A. Ern and J.L. Guermond. *Finite elements I: Approximation and interpolation*, volume 72. Springer, 2021.

[23] A. Ern and J.L. Guermond. *Finite elements II: Galerkin Approximation, Elliptic and Mixed PDEs*, volume 73. Springer, 2021.

[24] A. Ern and M. Vohralík. Polynomial-degree-robust a posteriori estimates in a unified setting for conforming, nonconforming, discontinuous galerkin, and mixed discretizations. *SIAM Journal on Numerical Analysis*, 53(2): 1058–1081, 2015.

[25] A. Ern and M. Vohralík. Flux reconstruction and a posteriori error estimation for discontinuous Galerkin methods on general nonmatching grids. *Comptes Rendus Mathematique*, 347(7):441–444, 2009. ISSN 1631-073X.

[26] A. Ern, S. Nicaise, and M. Vohralík. An accurate H(div) flux reconstruction for discontinuous Galerkin approximations of elliptic problems. *Comptes Rendus Mathematique*, 345(12):709–712, 2007.

[27] Alexandre Ern, Annette F. Stephansen, and Martin Vohralík. Guaranteed and robust discontinuous Galerkin a posteriori error estimates for convection–diffusion–reaction problems. *Journal of Computational and Applied Mathematics*, 234(1):114–130, 2010. ISSN 0377-0427.

[28] H. Fernando, C. Harder, D. Paredes, and F. Valentin. Numerical multiscale methods for a reaction-dominated model. *Computer Methods in Applied Mechanics and Engineering*, 201:228–244, 2012.

[29] A. T. A. Gomes, W. S. Pereira, and F. Valentin. The MHM method for linear elasticity on polytopal meshes. *IMA Journal of Numerical Analysis*, 43(4):2265–2298, 08 2022. ISSN 0272-4979.

[30] C. Harder and F. Valentin. Foundations of the MHM method. In G. R. Barrenechea, F. Brezzi, A. Cangiani, and E. H. Georgoulis, editors, *Building Bridges: Connections and Challenges in Modern Approaches to Numerical Partial Differential Equations*, Lecture Notes in Computational Science and Engineering, Edinburgh, 2016. Springer.

[31] C. Harder, D. Paredes, and F. Valentin. A family of multiscale hybrid-mixed finite element methods for the Darcy equation with rough coefficients. *J. Comput. Phys.*, 245:107–130, 2013.

[32] F. Hecht. New development in FreeFem++. *J. Numer. Math.*, 20(3-4): 251–265, 2012. ISSN 1570-2820.

[33] T. JR Hughes, G. R Feijó, L. Mazzei, and J.B. Quincy. The variational multiscale method—a paradigm for computational mechanics. *Computer methods in applied mechanics and engineering*, 166(1-2):3–24, 1998.

[34] O. A. Karakashian and F. Pascal. A posteriori error estimates for a discontinuous Galerkin approximation of second-order elliptic problems. *SIAM Journal on Numerical Analysis*, 41(6):2374–2399, 2003.

[35] A. Loula, F. Rochinha, and M. Murad. Higher-order gradient post-processings for second-order elliptic problems. *Computer Methods in Applied Mechanics and Engineering*, 128(3-4):361–381, 1995.

[36] A. Målqvist and D. Peterseim. *Numerical homogenization by localized orthogonal decomposition*, volume 5 of *SIAM Spotlights*. Society for Industrial and Applied Mathematics (SIAM), Philadelphia, PA, 2021. ISBN

978-1-611976-44-1.

[37] A.L. Madureira and M. Sarkis. Hybrid localized spectral decomposition for multiscale problems. *SIAM Journal on Numerical Analysis*, 59(2): 829–863, 2021.

[38] A. Malqvist and D. Peterseim. Localization of elliptic multiscale problems. *Math. Comp.*, 83(290):2583–2603, 2014.

[39] P. Oswald. On a bpx-preconditioner for P1 elements. *Computing (Wien. Print)*, 51(2):125–133, 1993.

[40] G.V. Pencheva, M. Vohralík, M.F. Wheeler, and T. Wildey. Robust a posteriori error control and adaptivity for multiscale, multinumerics, and mortar coupling. *SIAM Journal on Numerical Analysis*, 51(1):526–554, 2013.

[41] W. Prager and J. L. Synge. Approximations in elasticity based on the concept of function space. *Quarterly of Applied Mathematics*, 5(3):241–269, 1947.

[42] P.A. Raviart and J.M. Thomas. Primal hybrid finite element methods for 2nd order elliptic equations. *Math. Comp.*, 31(138):391–413, 1977.

[43] A. Veeser and R. Verfürth. Poincaré constants for finite element stars. *IMA Journal of Numerical Analysis*, 32(1):30–47, 05 2011. ISSN 0272-4979.

[44] M. Vlasák. On polynomial robustness of flux reconstructions. *Applications of Mathematics*, 65(2):153–172, 2020.

(GRB) Department of Mathematics and Statistics, University of Strathclyde, Glasgow, Scotland, gabriel.barrenechea@strath.ac.uk

(LM) Department of Mathematical and Computational Methods, LNCC, Petrópolis, RJ, Brazil larissam@posgrad.lncc.br

(WSP) Computational Science Center, National Renewable Energy Laboratory, CO, US wdasilv@nrel.gov

(FV) Department of Mathematical and Computational Methods, LNCC, Petrópolis, RJ, Brazil valentin@lncc.br